

# UCSF

## UC San Francisco Previously Published Works

### Title

1-BENZYLSPIRO[PIPERIDINE-4,1'-PYRIDO[3,4-b]indole] 'co-potentiators' for minimal function CFTR mutants.

### Permalink

<https://escholarship.org/uc/item/2jt1m0z8>

### Authors

Son, Jung-Ho  
Phuan, Puay-Wah  
Zhu, Jie S  
[et al.](#)

### Publication Date

2021

### DOI

10.1016/j.ejmech.2020.112888

Peer reviewed



Published in final edited form as:

*Eur J Med Chem.* 2021 January 01; 209: 112888. doi:10.1016/j.ejmech.2020.112888.

## 1-BENZYLSPIRO[PIPERIDINE-4,1'-PYRIDO[3,4-B]INDOLE] 'CO-POTENTIATORS' FOR MINIMAL FUNCTION CFTR MUTANTS

Jung-Ho Son<sup>†,1</sup>, Puay-Wah Phuan<sup>‡,1</sup>, Jie S. Zhu<sup>†,2</sup>, Elena Lipman<sup>†</sup>, Amy Cheung<sup>†</sup>, Ka Yi Tsui<sup>†</sup>, Dean J. Tantillo<sup>†</sup>, Alan S. Verkman<sup>‡</sup>, Peter M. Haggie<sup>‡,\*</sup>, Mark J. Kurth<sup>†,\*</sup>

<sup>†</sup>Department of Chemistry, University of California, Davis, CA, 95616, USA

<sup>‡</sup>Departments of Medicine & Physiology, University of California San Francisco, CA 94143, USA

### Abstract

We previously identified a spiro[piperidine-4,1-pyrido[3,4-b]indole] class of co-potentiators that function in synergy with existing CFTR potentiators such as VX-770 or GLGP1837 to restore channel activity of a defined subset of minimal function cystic fibrosis transmembrane conductance regulator (CFTR) mutants. Here, structure-activity studies were conducted to improve their potency over the previously identified compound, **20** (originally termed CP-A01). Targeted synthesis of 37 spiro[piperidine-4,1-pyrido[3,4-b]indoles] was generally accomplished using versatile two or three step reaction protocols with each step having high efficiency. Structure-activity relationship studies established that analog **2i**, with 6'-methoxyindole and 2,4,5-trifluorobenzyl substituents, had the greatest potency for activation of N1303K-CFTR, with EC<sub>50</sub> ~600 nM representing an ~17-fold improvement over the original compound identified in a small molecule screen.

### Graphical Abstract

\*Corresponding Authors: Mark J. Kurth, 1 Shields Avenue, University of California, Davis, CA 95616, USA, Phone: (530) 554-2145, Fax: (530) 752-8995, mjkurth@ucdavis.edu, and, Peter M. Haggie, 513 Parnassus Ave, University of California, San Francisco, CA 94143-0521, USA, Phone: (415) 476-8530, Fax: (415) 665-3847, peter.haggie@ucsf.edu.

#### AUTHOR CONTRIBUTIONS:

The manuscript was written by J.-H.S., P.-W.P., J.S.Z., K.Y.T., D.J.T., A.S.V., P.M.H. and M.J.K. Synthesis of substrates was performed by J.-H.S., J.S.Z., A.P.T. and C.K.K. Synthetic work was performed by J.-H.S., J.S.Z., E.L., and A.C. Computational studies were performed by K.Y.T. Biological data collection were performed by P.-W.P. All authors have given approval to the final version of the manuscript.

<sup>1</sup>The authors contributed equally to the study

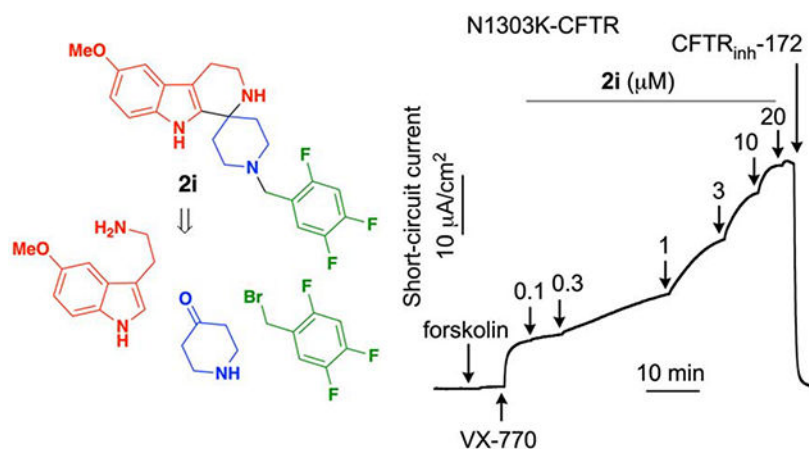
<sup>2</sup>Current Affiliation: Department of Chemistry, Stanford University, 337 Campus Drive, Standford, CA 94305

**Publisher's Disclaimer:** This is a PDF file of an unedited manuscript that has been accepted for publication. As a service to our customers we are providing this early version of the manuscript. The manuscript will undergo copyediting, typesetting, and review of the resulting proof before it is published in its final form. Please note that during the production process errors may be discovered which could affect the content, and all legal disclaimers that apply to the journal pertain.

Supporting Information: <sup>1</sup>H and <sup>13</sup>C NMR data (PDF) for all assayed compounds, molecular formula strings (CSV), mol2 files of all energetically relevant conformers, Boltzmann distribution analyses of **2a**, **2c**, **2e**, **4a-4c**, and **6a-6b**, and the computed H<sup>1</sup> coupling constants (*J*) for **6a** and **6b**. The Supporting Information is available free of charge on the ACS Publications website at DOI: #####.

#### Declaration of interests

The authors declare that they have no known competing financial interests or personal relationships that could have appeared to influence the work reported in this paper.



## Keywords

Cystic Fibrosis; CFTR; Modulator; Potentiator; N1303K-CFTR; c.3700A>G

## INTRODUCTION:

Cystic fibrosis transmembrane conductance regulator (CFTR) modulator therapy to restore defective folding and channel gating of CFTR mutants has been a major recent focus in cystic fibrosis (CF) drug development. CFTR modulators include ‘potentiators’, which restore channel gating, and ‘correctors’, which rescue misfolded CFTR to improve cell surface presentation [1]. Recently, a ‘triple combination’ therapy containing two correctors (tezacaftor / VX-661 and elxacaftor / VX-445) and ivacaftor (VX-770) was approved for CF subjects with at least one F508del-CFTR mutation [2–4]. With available potentiators and correctors it is anticipated that up to 90 % of CF subjects may have an efficacious CFTR modulator therapy [5].

There remains an unmet need to develop therapeutics for the remaining ~10% of CF subjects [5, 6]. We have described a novel approach that involves two potentiators, with the second potentiator called a ‘co-potentiator’, that function in synergy to increase chloride conductance for CFTR mutations found mainly in nucleotide binding domain 2 [7–9]. Recent high-throughput screening in cells expressing N1303K-CFTR identified four novel co-potentiator scaffolds, including spiro[piperidine-4,1-pyrido[3,4-b]indoles] and pyrazoloquinolines, some having sub-micromolar potency for activation of N1303K-CFTR when used together with VX-770 [9]. Herein, synthetic chemistry and structure-activity relationship studies were done to advance the spiro[piperidine-4,1-pyrido[3,4-b]indole] class of co-potentiators.

## RESULTS:

### Chemistry: General synthesis of spiro[piperidine-4,1-pyrido[3,4-b]indoles].

A synthetic scheme to enable investigation of co-potentiator structure-activity relationships (target analogs **1-6**) was devised as outlined in Scheme #1 for the efficient synthesis and

modification of the spiro[piperidine-4,1'-pyrido[3,4-*b*]indole] scaffold (**9**). Adapting technology developed by Mokrosz [10], commercial tryptamines (**8**) were condensed with *N*-alkylated (**11** → **12**; R<sup>2</sup>-X in CH<sub>2</sub>Cl<sub>2</sub> + K<sub>2</sub>CO<sub>3</sub>) [11, 12] piperidin-4-ones (**12** where n = 1) to directly deliver the targeted spiro[piperidine-4,1'-pyrido[3,4-*b*]indole] **9** by a classical Pictet–Spengler reaction [13, 14]. However, when preparing R<sup>2</sup> analogs of **9**, it proved more efficient to prepare unalkylated analog **10** [acetic acid-mediated condensation of tryptamine **8** with piperidin-4-one (**11**; n = 1)] and then subsequently perform selective *N*<sup>*l*</sup>-alkylation of **10** (R<sup>2</sup>-X in CH<sub>2</sub>Cl<sub>2</sub> + K<sub>2</sub>CO<sub>3</sub>) to give **9**. While the tryptamines employed in this chemistry were commercially available, these starting materials can be readily prepared in two steps by the Büchi/Mak method [15, 16] — 1*H*-indole nitro-olefination followed by exhaustive reduction with LiAlH<sub>4</sub> (**7** → **8**).

Figure 1 shows the synthesized analogs of the original hit spiro[piperidine-4,1'-pyrido[3,4-*b*]indole] **20** that were prepared in six rounds of synthetic study (synthesis rounds **r1** through **r6**). The co-potentiator activities (tested in an N1303K-CFTR expressing FRT cell model) of the synthesized analogs of **20** (10 μM/V<sub>MAX</sub> 100%) are summarized at the end of the chemistry description in Table 3, with further description of biological activity provided below (in the *Biology: Characterization of spiro[piperidine-4,1'-pyrido[3,4-*b*]indoles] co-potentiators* section).

The synthetic work began by preparing aryl analogs **1a-j** (synthesis round **r1**) to investigate the benzylic aryl moiety by appropriately *N*<sup>*l*</sup>-alkylating spiro[piperidine-4,1'-pyrido[3,4-*b*]indole] **10**. Of these first ten compounds, nine (**1b-j**) had a better EC<sub>50</sub> than **20** and two (**1c** and **1j**) showed improved V<sub>max</sub> (Table 3). The EC<sub>50</sub> and V<sub>MAX</sub> of the *N*<sup>*l*</sup>-3-chloro-2,4-difluorobenzyl analog **1j** (4.5 μM/120%) motivated us to next prepare a series of fluorobenzyl-analogs (**2a-i**) to examine the influence of fluoro-substitution patterns on co-potentiator activity. These round **r2** targets (Figure 1) were again prepared by selectively *N*<sup>*l*</sup>-alkylation of spiro[piperidine-4,1'-pyrido[3,4-*b*]indole] **10**. Increasing the number of fluorine atoms on the benzyl moiety (e.g., **2ac/2f/2h** with two fluorines versus **2d/2g/2i** with three and **2e** with five fluorines) improved the activity of these spirocycles. It was also noted that the positioning of the fluorine atoms on the benzyl moiety was important for maintaining both EC<sub>50</sub> and V<sub>MAX</sub> (Table 3: for example, compare **2a** versus **2b** and **2c**).

With results from synthetic rounds **r1** and **r2** in hand, the next objective (synthesis round **r3**, Figure 2) was to more broadly probe the requisite features of the *N*<sup>*l*</sup>-R<sup>3</sup>-substituent by preparation of analogs **3a-h**. Notably, deletion of R<sup>3</sup> (i.e., **3a** where R<sup>3</sup> = H) gave an inactive compound and lengthening the *N*<sup>*l*</sup>-aryl tether [–N(CH<sub>2</sub>)<sub>n</sub>R<sup>3</sup> from n = 1 (**1a**) to n = 2 (**3c**) or n = 3 (**3d**)] greatly reduced activity. Similarly, adding a methyl substituent to the CH<sub>2</sub> tether in **1a** (12.6 μM/V<sub>MAX</sub> 54%), giving **3b**, also reduced activity (**3b**: 20 μM/V<sub>MAX</sub> 100%). Replacing the phenyl moiety of **1a** with a furan ring (**3e**: 16.4 μM/V<sub>MAX</sub> 67%) reduced activity, while replacing the phenyl moiety of **1a** with a pyridyl ring to electronically mimic the perfluorophenyl moiety of compound **2e** was better tolerated with the nitrogen at position two (**3f**: 11.5 μM/V<sub>MAX</sub> 107%), but poorly tolerated with the nitrogen at position three (**3g**: 17 μM/V<sub>MAX</sub> 56%).

Having thoroughly investigated the *NI*-substituent in these spiro[piperidine-4,1'-pyrido[3,4-*b*]indoles], attention was next turned to a probe of the bisheterocyclic spiropiperidine moiety – synthesis round **r4** (Figure 1) targeting analogs **4a-d**. This work began with the preparation of spiroazepane, spiropyrrrolidine, and spiropiperidine analogs where the piperidine ring of **2a** was transformed into an azepine (**4a**), pyrrolidine (**4b**), and *N*-offset piperidine (**4c**) rings. These three analogs of **2a** were prepared by reaction of 2-(5-methoxy-1*H*-indol-3-yl)ethan-1-amine (**8** where R<sup>1</sup> = methoxy at C5) with the appropriate ketoamine (**12**), directly giving the targeted **2a** analogs **4a-c**. Interestingly, all three of these analogs were inactive. We next prepared piperidine ring-opened analogs truncated analog **4d**.

Conformational analysis was done to investigate possible mechanisms to explain the differences between active compounds **2a**, **2c** and **2e**, and inactive compounds **4a-4c**. We began with conformational searching using *Spartan10* (Wavefunction Inc., Irvine, CA). For the more flexible structures **4a** and **4c**, multiple runs of conformational search were performed and the results pooled. The conformational search runs were systematic and used the Merck Molecular Force Field (MMFF). All resulting conformers were subjected to single point energy calculations using PCM(chloroform)-B3LYP/6-31+G(d,p) [17–20]. Geometry optimizations were then performed on all conformers within 4 kcal/mol of the conformer with the lowest electronic energy, with the D3(BJ) dispersion correction [21, 22] included. All quantum chemical calculations were performed using *Gaussian16* (Gaussian Inc., Wallingford, CT). An implicit chloroform solvent was chosen for these calculations to simulate the polarity inside a general protein binding site [23]. Since **2a**, **2c**, **2e**, **4a-4c** contain fluorine atoms, the 6-31+G(d,p) basis set might not be sufficient for computing accurate energies; consequently, we also calculated energies for relevant conformers with PCM-(chloroform)-B3LYP-D3(BJ)/6-311+G(2d,2p). B3LYP/6-311+G(2d,2p) has been reported as a standard method for use with high electron affinity atoms, i.e., O and F [24].

Our conformational analysis suggested a trend distinguishing between active **2a**, **2c**, and **2e**, and inactive **4a-4c**. Figure 2 shows the optimized geometries of the lowest energy conformers B3LYP/6-31+G(d,p) for each structure. Most of the energetically relevant conformers of the active co-potentiators (i.e., **2a**, **2c**, and **2e**) have their benzene ring (*Ring i*) exposed for interaction, which we define as the “Open” form (Figure 2). Assuming that the CFTR binding site accommodates the Open form better and has residues in the vicinity to interact with the phenyl group of the co-potentiators, the Open conformers would allow for various interactions between the  $\pi$ -system and the CFTR interior. In contrast, most of the energetically relevant conformers for **4a-4c** have one face of *Ring i* interacting with the rest of the molecule, precluding protein interactions with it; we refer to these conformers as “Closed” (Figure 2).

Figure 3 shows the superposition of all optimized conformers within 4 kcal/mol of the lowest energy conformer for **2a**, **2c**, **2e**, and **4a-4c**. We aligned the conformers and calculated their RMSD values using an RMSD calculating tool from VMD [25]. In this case, we considered conformers to be unique if they have an RMSD value greater than 0.05 relative to other conformers. We then calculated the Boltzmann weighted averages for the Open and Closed conformers at room temperature. This allows us to determine the population of Open vs. Closed conformers for each structure, assuming all are in equilibrium

[26]. Table 1 summarizes the Boltzmann weighted averages for **2a**, **2c**, **2e**, and **4a-4c**. The results of this analysis emphasize the difference in conformational preferences for active and inactive structures

We also considered that these structures contain amines, which can be protonated in biological environments. Therefore, we performed conformational analysis on various protonated states for each structure as well. However, there were no consistent differences in conformational preferences for active and inactive structures. This analysis is complicated by the ability for amines to hydrogen bond with each other within each molecule (see Supporting Information for details), which may or may not occur in biologically relevant environs.

With exploration of the spiro[*piperidine-4,1'*-pyrido[3,4-*b*]indole] scaffold in hand with synthesis rounds **r1-r4**, we next turned to synthesis round **r5** where the indole moiety of scaffold **9** was probed with analogs **5a-e**. Spiro[*piperidine-4,1'*-pyrido[3,4-*b*]indoles] **5a-d** were prepared by reacting the appropriate tryptamine **8** with 1-(2,4-difluorobenzyl)piperidin-4-one (**12** in Scheme #1 where  $n = 1$  and  $R^2 = 2,4$ -difluorobenzyl). Whereas **5b** performed in a comparable manner to **20**, **5a** (8.2  $\mu\text{M}$ /100%) showed mild improvement, and **5c** (2.5  $\mu\text{M}$ /89%) and **5d** (2.4  $\mu\text{M}$ /100%) were approximately 4-fold more potent. Finally, we prepared indole *N*-methylated analog **5e** by employing 2-(5-methoxy-1-methyl-1*H*-indol-3-yl)ethan-1-amine in place of 2-(5-methoxy-1*H*-indol-3-yl)ethan-1-amine in a reaction with 1-(2,4-difluorobenzyl)piperidin-4-one (**8**  $\rightarrow$  **9** in Scheme #1). Compound **5e**, however, was inactive. In light of the structure-activity insights gained with synthetic rounds **r1-r5**, one final synthesis round (**r6**) was undertaken where targeting constrained spiro[*piperidine-4,1'*-pyrido[3,4-*b*]indole] analog **14** became a high priority in an attempt to address the question of whether there is a conformational requirement for activity vis-à-vis the *N'*-(benzyl) moiety. To address this issue, we set out to prepare **14**, a constrained analog of compound **2f**. *C*-Alkylation of diethyl acetamidomalonnate with 4-(bromomethyl)-1,2-difluorobenzene followed by ester hydrolysis/decarboxylation (Scheme #2) set the stage for a subsequent Pictet–Spengler reaction to delivered tetrahydroisoquinoline-3-carboxylic acid **13** [27]. Unfortunately, all attempts at the Pictet–Spengler failed – an apparent consequence of the electron deficient nature of the difluorophenyl ring. In light of this outcome, our constrained analog study was modified to instead target constrained analog **6** (the nor-fluoro analog of **14**). Commercially available 3-amino-4-phenylbutanoic acid (**15**) successfully participated in a Pictet–Spengler reaction to give **16** and subsequent esterification delivered methyl 2-(1,2,3,4-tetrahydroisoquinolin-3-yl)acetate (**17**). Michael addition to methyl acrylate delivered bis-ester intermediate **18**, which then underwent Dieckmann cyclization/decarboxylation to give ketone **19**. A second Pictet–Spengler reaction [28] of 2-(5-methoxy-1*H*-indol-3-yl)ethan-1-amine (**8** where  $R^1 = \text{methoxy at C5}$ ) with **19** gave the spiro[*piperidine-4,1'*-pyrido[3,4-*b*]indole] **6b** as the sole product – i.e., spiro[*piperidine-4,1'*-pyrido[3,4-*b*]indole] **6a** was not obtained.

To confirm the product is indeed **6b**, we performed quantum chemical  $^1\text{H}$  and  $^{13}\text{C}$  NMR calculations on both **6a** and **6b** (Figure 4). Both **6a** and **6b** were optimized using

SMD(chloroform)-B3LYP-D3(BJ)//6-31+G(d,p) [21, 22, 29]. Using the gauge-including atomic orbital (GIAO) [30] method, chemical shift calculations were performed with SMD(chloroform)-mPW1PW91/6-311+G(2d,p) [31] on conformers that are within 4 kcal/mol relative to the lowest energy conformer. The chemical shifts of these energetically relevant conformers were then averaged using Boltzmann distributions. This is a common procedure for computational NMR studies [30, 32, 33]. Linear scaling (using slope = -1.0533, intercept = 186.524) and (slope = -1.0936, intercept = 31.802) ([cheshirenmr.info](http://cheshirenmr.info)) was applied to computed isotropic shieldings to arrive at the  $^{13}\text{C}$  and  $^1\text{H}$  shifts, respectively. Due to the similarity in the calculated  $^1\text{H}$  shifts, coupling constants (Hz) were also calculated using the same methods to confirm the identity of some diagnostic  $^1\text{H}$  peaks (see SI for detail).

Table 2 shows the calculated chemical shifts for **6a** and **6b** and their deviations from the experimental shifts. Deviations within 6 ppm for  $^{13}\text{C}$  and 0.3 ppm for  $^1\text{H}$  shifts are considered acceptable [30, 32, 33]. Although the  $^{13}\text{C}$  chemical shifts for **6a** and **6b** are quite similar, the computed chemical shift at position C13 of **6a** deviates greatly from the experimental value, whereas all  $^{13}\text{C}$  shifts for **6b** are within the acceptable deviation range. Similarly, the deviations between the calculated  $^1\text{H}$  shifts for **6b** and the experimental shifts are within the accepted range, but the calculated chemical shifts at positions H15, H16, and H18 for **6a** have deviations greater than 0.3 ppm from the experimental shifts. Both  $^{13}\text{C}$  and  $^1\text{H}$  chemical shifts for **6b** have lower mean absolute deviations (MAD) compared to those for **6a** as well. We also compared the free energies of the lowest energy conformers of **6a** and **6b**; that for **6a** is ~2.3 kcal/mol higher than that for **6b** (Figure 4), consistent with formation of the thermodynamic product during synthesis.

The lowest energy conformer of **6b** resembles more closely the Closed conformers described above, but that of **6a** resembles the Open, i.e., where *Ring i* is available for interactions (Figure 5). Considering all conformers that are within 4 kcal/mol of the lowest energy conformers, Boltzmann distributions of open and closed forms of **6a** and **6b** were calculated (Figure 5). For **6a**, ~99.3% of conformers are predicted to be Open, while only 23.2% of conformers are predicted to be Open for **6b**. Therefore, we expect **6b** to have low activity at best, if our hypothesis that conformational bias is related to activity is correct. As predicted, **6b** was inactive when tested experimentally.

The structural determinants for activity of compound classes **1-6** are summarized in Figure 6. On the indole aryl 6-member ring ( $\text{R}^1$ ), 6'-methoxy (**2i**) was most potent, whereas substituents such as methoxy at 7' position (**5d**) showed decreased activity. Replacement of 6'-methoxy with bromo (**5b**) led to an inactive compound, although a chloro (**5c**) substitution was tolerated. At the indole nitrogen position ( $\text{R}^2$ ), hydrogen (**2i**) was required as methylation (**5e**) led to inactivity. For the benzyl moiety on the terminal piperidine ( $\text{R}^3$ ), we found 2,4,5-trifluorobenzyl (**2i**) to be best, di-halo-substituted moieties such as 2,4-dichlorobenzyl (**1d**) and 3-chloro-5-fluorobenzyl (**1e**) showed decreased activity, and methylene-linked heterocycles such as 2-furyl (**3e**), 2-pyridyl (**3f**), or 3-pyridyl (**3g**) were active, but less potent. Likewise, at  $\text{R}^3$ , lack of substitution on the terminal piperidine (**3a**), or compounds where the linked ring system is extended by longer linkers (**3c** and **3d**) were



also inactive. Finally, in terms of the bis-heterocyclic spiro-fused ring system, a piperidine ring (as in **2a**, **2i** and other compounds) was significantly more potent than an azepine (**4a**), and a pyrrolidine (**4b**), *N*-offset piperidine (**4c**) or ring-opened piperidine (**4d**) abolished activity.

Additional biological studies were performed for most potent compounds **2i** and **2e**. Copotentiator efficacy was initially determined by short-circuit current measurements in FRT cells expressing N1303K-CFTR in the presence of a transepithelial chloride gradient and with permeabilization of the basolateral cell membrane such that measured current directly reports CFTR channel activity. Representative data in Figure 7A show small increases in CFTR activity following addition of the cAMP agonist forskolin and the potentiator VX-770, followed by concentration-dependent increases in current following addition of the co-potentiators **2i** (*left*) and **2e** (*middle*), with EC<sub>50</sub> values  $0.6 \pm 0.2$  and  $2.1 \pm 0.3$   $\mu\text{M}$ , respectively (*right*). We previously defined potentiators as either class I compounds, including VX-770 and GLPG1837 [34], or class II compounds such as the arylsulphonamidepyrrolopyridine and spiro[piperidine-4,1-pyrido[3,4-b]indole] co-potentiators that probably bind at distinct sites on CFTR [9]. Indeed, structural and pharmacological studies have provided evidence that VX-770 and GLPG1837 bind to the same site on CFTR [35, 36]. Thus, as expected from our prior studies [9], N1303KCFTR-expressing FRT cells treated with forskolin and GLPG1837 had similar **2i** co-potentiator EC<sub>50</sub> of  $0.8 \pm 0.2$   $\mu\text{M}$  (Fig. 7B).

Compound **2i** was also tested on a second minimal function CFTR mutation, I1234del-CFTR, which is generated by the c.3700A>G mutation that results in deletion of 6 amino acids from the CFTR polypeptide (p.Ile1234\_Arg1239del-CFTR, hereafter termed I1234del-CFTR) due to introduction of a cryptic splice site in the CFTR transcript [37, 38]. As seen in Figure 7C, **2i** further activates I1234del-CFTR following forskolin and VX-770 to increase channel activity with EC<sub>50</sub> of  $0.7 \pm 0.2$   $\mu\text{M}$ , similar to that found with N1303K-CFTR. As expected, the R347P-CFTR mutant, which is mildly responsive to VX-770 but not responsive to arylsulphonamidepyrrolopyridine co-potentiators [9], was not activated by **2i** indicating that alternative mechanisms (such as increased cAMP signaling) are not responsible for activation of the N1303K- and I1234del-CFTR mutants (Fig. 7D).

The efficacy of **2i** was also tested in 16HBE14o- human bronchial epithelial cell models in which the endogenous CFTR gene was edited to contain the N1303K mutation (16HBEge-N1303K) or the I1234del mutation (16HBEge-I1234del) [38, 39]. As shown in N1303K- (Fig. 8A) and I1234del-CFTR (Fig. 8B) expressing 16HBE14o- cells, addition of forskolin and then VX-770 produced limited channel activity. However, subsequent addition of **2i** produced CFTR<sub>inh-172</sub>-inhibitable responses of  $16.1 \pm 0.4$   $\mu\text{A}/\text{cm}^2$  in N1303K- (Fig. 8A) and  $6.1 \pm 0.1$   $\mu\text{A}/\text{cm}^2$  in I1234del-CFTR (Fig. 8B) expressing cells, approximately 6-fold and 2-fold greater than that produced by VX-770 alone.

## CONCLUSIONS:

This study extends our prior work that identified a novel class of CFTR modulators, termed co-potentiators, that act in synergy with existing potentiators such as VX-770 and



GLPG1837 to increase chloride channel function of CFTR mutants [7–9]. The objective of this study was to optimize spiro[piperidine-4,1-pyrido[3,4-b]indoles] co-potentiators previously identified in a high-throughput screen [9]. A straightforward, high yielding synthetic strategy was developed to investigate structure-activity relationships. In total, 37 spiro[piperidine-4,1-pyrido[3,4-b]indoles] were synthesized to investigate the consequences of altering the indole and benzyl moieties. Analogs of the original spiro[piperidine-4,1'-pyrido[3,4-*b*]indole] compound **20** were prepared in six rounds of synthetic studies (synthesis rounds **r1** through **r6**) starting from commercial tryptamines (**8**). These were condensed with *N*-alkylated piperidin-4-ones (**12**) to directly deliver the targeted spiro[piperidine-4,1'-pyrido[3,4-*b*]indole] **9** by a classical Pictet–Spengler reaction. When preparing R<sup>2</sup> analogs of **9**, it proved more efficient to prepare unalkylated analog **10** [acetic acid-mediated condensation of tryptamine **8** with piperidin-4-one (**11**)] and then subsequently perform selective *N*<sup>1</sup>-alkylation of **10** (R<sup>2</sup>-X in CH<sub>2</sub>Cl<sub>2</sub> + K<sub>2</sub>CO<sub>3</sub>) to give **9**.

It is estimated that up to 90% of CF subjects will benefit from available CFTR modulators including Trikafta [5], with ~10% of CF subjects not benefitted. For co-potentiators, we have demonstrated efficacy for several NBD2 mutants including the missense mutant N1303K, the c.3700A>G splicing mutant, and truncated CFTR protein generated by the premature termination codon (PTC) W1282X [7–9]. In addition, albeit to a lesser degree, channel activity of the VX-770-responsive G551D mutation can be further augmented by co-potentiators [7]. Co-potentiators may be beneficial for some PTCs if sufficient transcript is present, or in combination with future read-through or other therapies [40].

In summary, spiro[piperidine-4,1-pyrido[3,4-b]indoles] represent an evolvable CFTR co-potentiator scaffold with nanomolar potency that in synergy with existing potentiators activates certain CF-causing CFTR mutations. The expansion of spiro[piperidine-4,1-pyrido[3,4-b]indole] structure activity relationships may yield insight into the binding site of co-potentiators through computational or structural approaches [35, 36], as well as subsequent rational compound optimization.

## MATERIALS AND METHODS:

### General Experimental:

All compounds described in this manuscript have 95% purity. The analytical method used to determine purity was <sup>1</sup>H NMR (see the accompanying Supporting Information file which provides the <sup>1</sup>H- and <sup>13</sup>C-NMR for the thirty-seven compounds assayed) and HPLC/HRMS. For HRMS analysis, samples were analyzed by flow-injection analysis into a Thermo Fisher Scientific LTQ Orbitrap (San Jose, CA) operated in the centroided mode. Samples were injected into a mixture of 50% MeOH/H<sub>2</sub>O and 0.1% formic acid at a flow of 0.2 mL/min. Source parameters were 5.5kV spray voltage, capillary temperature of 275 °C and sheath gas setting of 20. Spectral data were acquired at a resolution setting of 100,000 FWHM with the lockmass feature, which typically results in a mass accuracy <2ppm.

**Cell culture:**

Fischer Rat Thyroid (FRT) cells transfected to stably express N1303K-CFTR, I1234del-CFTR and R347P-CFTR were cultured as described [8, 9]. Gene-edited 16HBE14o-cells expressing N1303K-CFTR were provided by CFFT lab and were cultured as described [39]. Gene-edited 16HBE14o- cells expressing I1234del-CFTR were a generous gift of Dr. Christine Bear (The Hospital for Sick Children, Toronto, Canada) and were cultured as described [38].

**Short-circuit current measurement.**

Short-circuit current measurements were made essentially as described in prior studies [8, 9]. In brief, measurements were made using a DVC-1000 voltage clamp (World Precision Instruments Inc., Sarasota, FL), cells were cultured on Snapwell clear permeable supports (Corning), and experiments were performed using  $\text{HCO}_3^-$ -buffered solutions at 37 °C. For studies using FRT cells the basolateral membrane was permeabilized with 250  $\mu\text{g/ml}$  amphotericin B and experiments were done with a chloride gradient. For 16HBE14o- gene-edited cells experiments were done with a chloride gradient using Hepes-buffered solutions.

**Statistical analysis.**

Data are presented as mean  $\pm$  S.E.M. Comparisons between two groups were performed using the unpaired Student's t-test.  $P < 0.05$  was considered as statistically significant.

**General experimental for the synthesis of 2',3',4',9'-tetrahydrospiro[piperidine-4,1'-pyrido[3,4-*b*]indoles] (8  $\rightarrow$  9):**

Tryptamine (**8**, 0.6 mmol) was mixed with glacial acetic acid (3 mL) in a 10 mL vial and stirred with a magnetic stirrer. Corresponding ketone (**12**, 0.5 mmol) was added and the vial was sealed with a plastic cap. The vial was heated at 100 °C for 16 h in an oil bath. After cooling, the solution was diluted with water (~20 mL) and neutralized by adding 4 M HCl. The product was extracted with dichloromethane, and the organic solution was washed with water, brine and dried over magnesium sulfate. The solvent was removed in vacuo, and the product was purified by using flash column chromatography (2.5 % MeOH/DCM).

**General experimental for the synthesis of *N*-alkylated piperidin-4-one analogs (11  $\rightarrow$  12):**

4-Piperidone hydrochloride (**11**, 5 mmol) was mixed with 25 mL of dichloromethane in an Erlenmeyer flask. Small amount of methanol (5 drops) was added and benzyl bromide (2.5 mmol) and potassium carbonate (5 mmol) was added. The mixture was stirred at RT for 16h. Water was added to the reaction mixture and the product was extracted with dichloromethane. The extracted organic solution was washed with water, brine, and dried over magnesium sulfate. The solvent was removed in vacuo, and the product was purified by using flash column chromatography (2.5 % MeOH/DCM).

**General experimental for the synthesis of 2',3',4',9'-tetrahydrospiro[piperidine-4,1'-pyrido[3,4-*b*]indoles] (10  $\rightarrow$  9):**

Compound **3a** (0.5 mmol) was mixed with 5 mL of dichloromethane in a small vial. Small amount of methanol (1 drop) was added for better solubility, and benzyl bromide (0.5 mmol)

and potassium carbonate (1.5 mmol) was added. The vial was capped, and the mixture was stirred at RT for 16h. Water was added to the reaction mixture and the product was extracted with dichloromethane. The extracted organic solution was washed with water, brine, and dried over magnesium sulfate. The solvent was removed in vacuo, and the product was purified by using flash column chromatography (2.5 % MeOH/DCM).

**General experimental for the synthesis of 2',3',4',9'-tetrahydrospiro[piperidine-4,1'-pyrido[3,4-*b*]indoles] (8 → 10):**

5-methoxytryptamine (**8**, 25 mmol) was mixed with glacial acetic acid (20 mL) in a round bottom flask. 4-piperidone hydrochloride (**11**, 25 mmol) was added and the solution was heated at 100 °C for 16 h in an oil bath with stirring. The solution was cooled to RT and diluted with water (100 mL) and neutralized with 4 M NaOH. Tan precipitate formed upon standing within an hour. The precipitate was filtered and washed with water and air dried. Yield = 54%.

**General experimental for the synthesis of tryptamines (7 → 8):**

1-Dimethylamino-2-nitroethylene (3 mmol) was mixed in TFA (4 mL) in a vial. Substituted indole (**7**, 3.6 mmol) was dissolved in dichloromethane (3 mL) separately and added. The mixture was stirred at RT for 2 h and the solution was diluted with dichloromethane. The organic solution was washed with water, brine and dried over magnesium sulfate. Solvent was removed in vacuo and purified by using flash column chromatography (50 % EtOAc/hexane). LiAlH<sub>4</sub> (12 mmol) was mixed with THF (75 mL) and cooled at -78 °C and stirred. The product from the previous step dissolved in small amount of THF was added dropwise and the mixture was stirred overnight with slowly warming to RT. The reaction mixture was cooled in an ice bath and quenched with water and 4 M NaOH solution. Organic solvent was removed in vacuo and the product was extracted with dichloromethane. The extracted solution was washed with water, brine, and dried over magnesium sulfate. The solvent was removed in vacuo, and the product was directly used.

**Synthesis of 2-(1,2,3,4-tetrahydroisoquinolin-3-yl)acetic acid (16):**

L-β-homophenylalanine hydrochloride (1 g, 4.6 mmol) was mixed with concentrated HCl (10 mL) in a round bottom flask and formaldehyde (37% aqueous solution, 4 mL, 49 mmol) was added. The mixture was refluxed at 100 °C for 3h with stirring. After cooling, solvent was removed in vacuo to obtain off-white solid in quantitative yield, which was used for the next step without purification.

**Synthesis of methyl 2-(1,2,3,4-tetrahydroisoquinolin-3-yl)acetate (17):**

**16** (1g, 4.3 mmol) was placed in a round bottom flask. Trimethylchlorosilane 1.26 mL was added dropwise with stirring, then methanol (20 mL) was added and stirred for 2 h. Solvent was removed in vacuo and dried in vacuum. The solid product was used for the next step without purification.

**Synthesis of methyl 3-(3-(2-methoxy-2-oxoethyl)-3,4-dihydroisoquinolin-2(1H)-yl)propanoate (18):**

**17** (0.62g, 3 mmol) was dissolved in dichloromethane (30 mL) and trifluoroacetic acid (3 mL) was added and stirred briefly. Solvent was removed in vacuo and the resulting oil was extracted with ethyl acetate. The organic solution was washed with saturated sodium bicarbonate solution, and the solvent was removed in vacuo. To the resulting oil, methyl acrylate (10 mL) was added and refluxed at 80 °C overnight. Solvent was removed in vacuo, and the product was used without purification for the next step.

**Synthesis of 1,3,4,6,11,11a-hexahydro-2H-pyrido[1,2-b]isoquinolin-2-one (19):**

Lithium diisopropylamide (LDA, 1M solution in THF/hexane, 10 mL) was cooled at -78 °C under N<sub>2</sub> atmosphere. Crude product of **18** was dissolved in anhydrous THF (8 mL) under N<sub>2</sub> atmosphere and added to the LDA solution by syringe. The mixture solution was stirred at -78 °C for 1 h. Concentrated HCl (0.8 mL) was added to the solution and brought to RT. Solvent was removed in vacuo then H<sub>2</sub>O (25 mL) and concentrated HCl (25 mL) was added, and the solution was refluxed at 100 °C overnight. After cooling, the solution was basified by adding solid K<sub>2</sub>CO<sub>3</sub> portion wise. The product was extracted with diethyl ether and the organic layer was washed with water, brine and dried with magnesium sulfate. Crude product (220 mg) was used for the next step without purification.

Synthesis of (2*R*,11*aS*)-6'-methoxy-1,2',3,3',4,4',6,9',11,11*a*-decahydrospiro[pyrido[1,2-*b*]isoquinoline-2,1'-pyrido[3,4-*b*]indole] (**6b**): Crude **19** (220 mg, 1.1 mmol) was placed in a glass vial and 5-methoxytryptamine (250 mg, 1.3 mmol) was added and glacial acetic acid (3 mL) was added. The vial was capped and heated at 100 °C overnight. After cooling, the solution was diluted with water (~20 mL) and neutralized by adding 4 M HCl. The product was extracted with dichloromethane, and the organic solution was washed with water, brine and dried over magnesium sulfate. The solvent was removed in vacuo, and the product was purified by using flash column chromatography (2.5 % MeOH/DCM).

**1-Benzyl-6'-methoxy-2',3',4',9'-tetrahydrospiro[piperidine-4,1'-pyrido[3,4-*b*]indole] (1a).**

Yield = 152 mg (84 %). <sup>1</sup>H NMR (400 MHz, CDCl<sub>3</sub>) δ 8.30 (d, *J* = 35.1 Hz, 1H), 7.43 (d, *J* = 7.2 Hz, 2H), 7.39 – 7.27 (m, 3H), 7.22 (d, *J* = 8.7 Hz, 1H), 6.96 (d, *J* = 2.5 Hz, 1H), 6.82 (dt, *J* = 8.9, 1.8 Hz, 1H), 3.87 (s, 3H), 3.69 (s, 2H), 3.15 (t, *J* = 5.6 Hz, 2H), 2.96 – 2.77 (m, 2H), 2.77 – 2.53 (m, 4H), 2.25 (td, *J* = 13.4, 4.4 Hz, 2H), 1.79 (d, *J* = 13.7 Hz, 2H). <sup>13</sup>C NMR (101 MHz, CDCl<sub>3</sub>) δ 153.99, 140.62, 136.72, 130.69, 129.67, 128.46, 127.64, 127.60, 111.62, 111.44, 108.42, 100.50, 63.09, 56.07, 50.52, 48.80, 39.16, 35.86, 23.23. HRMS (ESI) *m/z* for C<sub>23</sub>H<sub>28</sub>N<sub>3</sub>O [M+H]. calcd 362.2232, found 362.2229.

**1-(2-Fluoro-4-nitrobenzyl)-6'-methoxy-2',3',4',9'-tetrahydrospiro[piperidine-4,1'-pyrido[3,4-*b*]indole] (1b).**

Yield = 119 mg (56 %). <sup>1</sup>H NMR (400 MHz, CDCl<sub>3</sub>) δ 7.92 (s, 1H), 7.57 (td, *J* = 5.2, 2.8 Hz, 2H), 7.32 – 7.18 (m, 2H), 6.95 (d, *J* = 2.4 Hz, 1H), 6.82 (dd, *J* = 8.7, 2.5 Hz, 1H), 3.86 (d, *J* = 11.3 Hz, 5H), 3.14 (t, *J* = 5.7 Hz, 2H), 2.69 (t, *J* = 5.6 Hz, 2H), 2.64 – 2.54 (m, 4H), 2.01 (ddd, *J* = 13.8, 10.3, 6.5 Hz, 2H), 1.79 – 1.71 (m, 2H). <sup>13</sup>C NMR (101 MHz, CDCl<sub>3</sub>) δ

162.37, 159.88, 154.03, 150.11 (d,  $J_{C-F}$  = 8.4 Hz), 140.70, 132.64 (d,  $J_{C-F}$  = 7.8 Hz), 130.61, 130.06 (d,  $J_{C-F}$  = 3.7 Hz), 127.72, 119.34 (d,  $J_{C-F}$  = 20.7 Hz), 112.21 (d,  $J_{C-F}$  = 26.4 Hz), 111.51 (d,  $J_{C-F}$  = 7.6 Hz), 108.51, 100.53, 58.88, 56.06, 50.58, 48.83, 39.07, 36.37, 23.15. HRMS (ESI)  $m/z$  for  $C_{23}H_{26}FN_4O_3$  [M+H]. calcd 425.1989, found 425.1978.

**1-(5-Chloro-2-nitrobenzyl)-6'-methoxy-2',3',4',9'-tetrahydrospiro[piperidine-4,1'-pyrido[3,4-b]indole] (1c).**

Yield = 128 mg (58 %).  $^1H$  NMR (400 MHz,  $CDCl_3$ )  $\delta$  7.90 (s, 1H), 7.83 (d,  $J$  = 8.6 Hz, 1H), 7.68 (d,  $J$  = 2.3 Hz, 1H), 7.39 (dd,  $J$  = 8.6, 2.3 Hz, 1H), 7.23 (d,  $J$  = 8.7 Hz, 1H), 6.96 (d,  $J$  = 2.4 Hz, 1H), 6.83 (dd,  $J$  = 8.8, 2.4 Hz, 1H), 3.87 (d,  $J$  = 2.6 Hz, 5H), 3.16 (t,  $J$  = 5.7 Hz, 2H), 2.70 (t,  $J$  = 5.7 Hz, 2H), 2.67 – 2.61 (m, 4H), 2.08 – 1.98 (m, 2H), 1.78 (d,  $J$  = 13.5 Hz, 2H), 1.29 (s, 1H).  $^{13}C$  NMR (101 MHz,  $CDCl_3$ )  $\delta$  154.05, 147.99, 140.57, 138.85, 136.69, 130.80, 130.62, 127.99, 127.72, 125.99, 111.55, 111.52, 108.55, 100.54, 59.06, 56.07, 50.59, 48.95, 39.08, 36.39, 23.11. HRMS (ESI)  $m/z$  for  $C_{23}H_{26}ClN_4O_3$  [M+H]. calcd 441.1693, found 441.1685.

**1-(2,4-Dichlorobenzyl)-6'-methoxy-2',3',4',9'-tetrahydrospiro[piperidine-4,1'-pyrido[3,4-b]indole] (1d).**

Yield = 156 mg (72 %).  $^1H$  NMR (400 MHz,  $CDCl_3$ )  $\delta$  7.92 (s, 1H), 7.47 (d,  $J$  = 8.3 Hz, 1H), 7.41 (d,  $J$  = 2.2 Hz, 1H), 7.27 – 7.15 (m, 2H), 6.97 (d,  $J$  = 2.4 Hz, 1H), 6.83 (dd,  $J$  = 8.7, 2.4 Hz, 1H), 3.88 (s, 3H), 3.68 (s, 2H), 3.17 (t,  $J$  = 5.6 Hz, 2H), 2.88 – 2.52 (m, 6H), 2.28 – 2.00 (m, 2H), 1.80 (d,  $J$  = 14.3 Hz, 3H).  $^{13}C$  NMR (101 MHz,  $CDCl_3$ )  $\delta$  154.05, 140.85, 135.06, 134.79, 133.21, 131.70, 130.57, 129.27, 127.77, 126.95, 111.49, 111.47, 108.59, 100.56, 59.02, 56.08, 50.58, 48.93, 39.12, 36.44, 23.22. HRMS (ESI)  $m/z$  for  $C_{23}H_{26}Cl_2N_3O$  [M+H]. calcd 430.1453, found 430.1447.

**1-(3-Chloro-5-fluorobenzyl)-6'-methoxy-2',3',4',9'-tetrahydrospiro[piperidine-4,1'-pyrido[3,4-b]indole] (1e).**

Yield = 187 mg (91 %).  $^1H$  NMR (800 MHz,  $CDCl_3$ )  $\delta$  8.09 (s, 1H), 7.25 – 7.15 (m, 2H), 7.08 – 7.00 (m, 2H), 6.98 (d,  $J$  = 2.7 Hz, 1H), 6.84 (dd,  $J$  = 8.7, 2.5 Hz, 1H), 3.89 (s, 3H), 3.54 (s, 2H), 3.15 (t,  $J$  = 5.7 Hz, 2H), 2.71 (q,  $J$  = 5.2 Hz, 4H), 2.61 – 2.46 (m, 2H), 2.10 (td,  $J$  = 13.4, 4.2 Hz, 2H), 1.83 – 1.69 (m, 2H).  $^{13}C$  NMR (201 MHz,  $CDCl_3$ )  $\delta$  163.35, 162.12, 154.01, 142.79 (d,  $J_{C-F}$  = 7.8 Hz), 140.84, 134.76 (d,  $J_{C-F}$  = 10.4 Hz), 130.65, 127.76, 124.82 (d,  $J_{C-F}$  = 2.9 Hz), 114.87 (d,  $J_{C-F}$  = 24.9 Hz), 114.27 (d,  $J_{C-F}$  = 21.4 Hz), 111.52 (d,  $J_{C-F}$  = 18.3 Hz), 108.56, 100.57, 62.25, 56.07, 50.58, 48.91, 39.09, 36.33, 23.21. HRMS (ESI)  $m/z$  for  $C_{23}H_{26}ClFN_3O$  [M+H]. calcd 414.1748, found 414.1740.

**1-(3-Chloro-2,6-difluorobenzyl)-6'-methoxy-2',3',4',9'-tetrahydrospiro[piperidine-4,1'-pyrido[3,4-b]indole] (1f).**

Yield = 183 mg (85 %).  $^1H$  NMR (400 MHz,  $CDCl_3$ )  $\delta$  8.34 (s, 1H), 7.30 (h,  $J$  = 5.4 Hz, 1H), 7.16 (d,  $J$  = 8.8 Hz, 1H), 6.96 (d,  $J$  = 2.6 Hz, 1H), 6.87 – 6.72 (m, 2H), 3.88 (s, 3H), 3.76 (s, 2H), 3.13 (t,  $J$  = 5.7 Hz, 2H), 2.79 (d,  $J$  = 11.4 Hz, 2H), 2.73 – 2.56 (m, 4H), 2.10 (td,  $J$  = 13.3, 4.7 Hz, 2H), 1.77 (d,  $J$  = 12.8 Hz, 2H).  $^{13}C$  NMR (101 MHz,  $CDCl_3$ )  $\delta$  160.35 (dd,  $J_{C-F}$  = 248.7, 7.0 Hz), 157.24 (dd,  $J_{C-F}$  = 250.2, 8.4 Hz), 153.93, 140.88, 130.71, 129.69 (d,

$J_{C-F} = 9.5$  Hz), 127.70, 116.55 (dd,  $J_{C-F} = 19.1, 4.0$  Hz), 114.91 (t,  $J_{C-F} = 20.2$  Hz), 111.83 (dd,  $J_{C-F} = 24.6, 4.0$  Hz), 111.63, 111.33, 108.38, 100.52, 56.06, 50.44, 49.43, 48.31, 39.10, 36.18, 23.20. HRMS (ESI)  $m/z$  for  $C_{23}H_{25}ClF_2N_3O$  [M+H]. calcd 432.1654, found 432.1655.

**1-(2-Chlorobenzyl)-6'-methoxy-2',3',4',9'-tetrahydrospiro[piperidine-4,1'-pyrido[3,4-b]indole] (1g).**

Yield = 126 mg (64 %)  $^1H$  NMR (400 MHz,  $CDCl_3$ )  $\delta$  8.13 (s, 1H), 7.54 (dd,  $J = 7.4, 2.3$  Hz, 1H), 7.41 (dd,  $J = 7.5, 1.9$  Hz, 1H), 7.26 (qd,  $J = 7.4, 6.6, 2.1$  Hz, 2H), 7.22 – 7.13 (m, 1H), 6.98 (d,  $J = 2.7$  Hz, 1H), 6.84 (dd,  $J = 8.8, 2.6$  Hz, 1H), 3.89 (s, 3H), 3.74 (s, 2H), 3.17 (t,  $J = 5.7$  Hz, 2H), 2.82 (dt,  $J = 12.1, 3.7$  Hz, 2H), 2.74 – 2.58 (m, 4H), 2.14 (td,  $J = 13.1, 4.6$  Hz, 2H), 1.80 (dd,  $J = 13.9, 2.4$  Hz, 2H).  $^{13}C$  NMR (101 MHz,  $CDCl_3$ )  $\delta$  154.00, 140.97, 135.92, 134.57, 131.10, 130.64, 129.58, 128.37, 127.75, 126.67, 111.57, 111.40, 108.45, 100.56, 59.64, 56.10, 50.65, 48.97, 39.16, 36.35, 23.22. HRMS (ESI)  $m/z$  for  $C_{23}H_{27}ClN_3O$  [M+H]. calcd 396.1843, found 396.1836.

**1-(4-Bromo-3-fluorobenzyl)-6'-methoxy-2',3',4',9'-tetrahydrospiro[piperidine-4,1'-pyrido[3,4-b]indole] (1h).**

Yield = 155 mg (68 %)  $^1H$  NMR (400 MHz,  $CDCl_3$ )  $\delta$  8.00 (s, 1H), 7.48 (dd,  $J = 8.2, 7.1$  Hz, 1H), 7.21 (dd,  $J = 9.1, 2.9$  Hz, 2H), 7.07 – 6.93 (m, 2H), 6.85 (dd,  $J = 8.7, 2.5$  Hz, 1H), 3.89 (s, 3H), 3.54 (s, 2H), 3.17 (t,  $J = 5.7$  Hz, 2H), 2.79 – 2.65 (m, 4H), 2.63 – 2.44 (m, 2H), 2.10 (td,  $J = 13.2, 12.8, 4.4$  Hz, 2H), 1.88 – 1.70 (m, 2H).  $^{13}C$  NMR (101 MHz,  $CDCl_3$ )  $\delta$  160.33, 157.87, 154.04, 140.89, 140.84 (d,  $J_{C-F} = 6.6$  Hz), 133.17, 130.64, 127.80, 125.78 (d,  $J_{C-F} = 3.3$  Hz), 116.90 (d,  $J_{C-F} = 22.0$  Hz), 111.51 (d,  $J_{C-F} = 4.4$  Hz), 108.62, 107.20 (d,  $J_{C-F} = 20.9$  Hz), 100.61, 62.20, 56.10, 50.62, 48.92, 39.11, 36.42, 23.23. HRMS (ESI)  $m/z$  for  $C_{23}H_{26}BrFN_3O$  [M+H]. calcd 458.1243, found 458.1239.

**1-(4-Bromo-2-fluorobenzyl)-6'-methoxy-2',3',4',9'-tetrahydrospiro[piperidine-4,1'-pyrido[3,4-b]indole] (1i).**

Yield = 190 mg (83 %)  $^1H$  NMR (400 MHz,  $CDCl_3$ )  $\delta$  8.59 (s, 1H), 7.24 (t,  $J = 8.1$  Hz, 1H), 7.15 (dd,  $J = 7.9, 2.6$  Hz, 3H), 6.98 (d,  $J = 2.6$  Hz, 1H), 6.81 (dd,  $J = 8.7, 2.5$  Hz, 1H), 3.88 (s, 3H), 3.60 (s, 2H), 3.14 (t,  $J = 5.7$  Hz, 2H), 2.72 (q,  $J = 7.2, 5.7$  Hz, 4H), 2.59 (td,  $J = 12.1, 2.5$  Hz, 2H), 2.10 (td,  $J = 13.5, 4.6$  Hz, 2H), 1.69 (s, 2H).  $^{13}C$  NMR (101 MHz,  $CDCl_3$ )  $\delta$  162.50, 160.00, 153.93, 140.87, 132.96 (d,  $J_{C-F} = 5.1$  Hz), 130.73, 127.72, 127.29 (d,  $J_{C-F} = 3.7$  Hz), 123.77 (d,  $J_{C-F} = 15.0$  Hz), 121.33 (d,  $J_{C-F} = 9.5$  Hz), 119.03 (d,  $J_{C-F} = 25.3$  Hz), 111.47 (d,  $J_{C-F} = 17.2$  Hz), 108.44, 100.56, 56.08, 55.35, 50.50, 48.72, 39.13, 36.03, 23.25. HRMS (ESI)  $m/z$  for  $C_{23}H_{26}BrFN_3O$  [M+H]. calcd 458.1243, found 458.1228.

**1-(3-Chloro-2,4-difluorobenzyl)-6'-methoxy-2',3',4',9'-tetrahydrospiro[piperidine-4,1'-pyrido[3,4-b]indole] (1j).**

Yield = 124 mg (58 %)  $^1H$  NMR (400 MHz,  $CDCl_3$ )  $\delta$  8.10 (s, 1H), 7.36 – 7.24 (m, 1H), 7.17 (s, 1H), 7.01 – 6.87 (m, 2H), 6.83 (dd,  $J = 8.7, 2.5$  Hz, 1H), 3.88 (s, 3H), 3.65 (s, 2H), 3.15 (t,  $J = 5.7$  Hz, 2H), 2.80 – 2.66 (m, 4H), 2.60 (td,  $J = 11.9, 2.6$  Hz, 2H), 2.10 (td,  $J = 13.4, 4.6$  Hz, 2H), 1.87 – 1.67 (m, 2H).  $^{13}C$  NMR (101 MHz,  $CDCl_3$ )  $\delta$  158.08 (dd,  $J_{C-F} =$



250.1, 2.9 Hz), 157.44 (d,  $J_{C-F}$  = 251.6, 2.9 Hz), 154.01, 140.77, 130.62, 129.34 (dd,  $J_{C-F}$  = 9.0, 5.7 Hz), 127.74, 121.95 (dd,  $J_{C-F}$  = 15.0, 4.0 Hz), 111.50, 111.46, 111.44 (dd,  $J_{C-F}$  = 20.6, 4.4 Hz), 109.77 (t,  $J_{C-F}$  = 21.3 Hz), 108.58, 100.56, 56.06, 55.41, 50.51, 48.65, 39.10, 36.27, 23.21. HRMS (ESI)  $m/z$  for  $C_{23}H_{25}ClF_2N_3O$  [M+H]. calcd 432.1654, found 432.1646.

**1-(2,4-Difluorobenzyl)-6'-methoxy-2',3',4',9'-tetrahydrospiro[piperidine-4,1'-pyrido[3,4-b]indole] (2a).**

Yield = 138 mg (70 %)  $^1H$  NMR (400 MHz,  $CDCl_3$ )  $\delta$  7.85 (s, 1H), 7.37 (q,  $J$  = 7.9 Hz, 1H), 7.18 (d,  $J$  = 8.7 Hz, 1H), 6.94 (s, 1H), 6.82 (ddt,  $J$  = 14.4, 8.8, 5.4 Hz, 3H), 3.85 (s, 3H), 3.61 (s, 2H), 3.13 (t,  $J$  = 5.7 Hz, 2H), 2.75 (d,  $J$  = 11.4 Hz, 2H), 2.67 (t,  $J$  = 5.8 Hz, 2H), 2.57 (t,  $J$  = 11.7 Hz, 2H), 2.07 (td,  $J$  = 13.2, 4.3 Hz, 2H), 1.79 (s, 2H).  $^{13}C$  NMR (101 MHz,  $CDCl_3$ )  $\delta$ , 161.14 – 154.80 (m), 140.93 – 128.43 (m), 120.82 (dd,  $J$  = 14.8, 3.9 Hz), 111.57 – 108.50 (m), 103.92 – 22.26 (m).  $^{13}C$  NMR (101 MHz,  $CDCl_3$ )  $\delta$  163.05 (dd,  $J_{C-F}$  = 77.9, 11.9 Hz), 160.58 (dd,  $J_{C-F}$  = 79.0, 12.0 Hz), 154.90, 154.04, 140.83, 132.40 (dd,  $J_{C-F}$  = 9.6, 6.2 Hz), 130.53, 128.52, 127.75, 120.82 (dd,  $J_{C-F}$  = 14.8, 3.9 Hz), 111.04 (dd,  $J_{C-F}$  = 20.9, 3.7 Hz), 108.60, 103.56 (t,  $J_{C-F}$  = 25.8 Hz), 100.54, 56.72, 56.05, 55.16, 51.90, 50.54, 48.64, 40.07, 39.10, 37.28, 36.37, 23.22, 22.36. HRMS (ESI)  $m/z$  for  $C_{23}H_{26}F_2N_3O$  [M+H]. calcd 398.2044, found 398.2036.

**1-(2,5-Difluorobenzyl)-6'-methoxy-2',3',4',9'-tetrahydrospiro[piperidine-4,1'-pyrido[3,4-b]indole] (2b).**

Yield = 173 mg (87 %)  $^1H$  NMR (400 MHz,  $CDCl_3$ )  $\delta$  8.12 – 7.83 (m, 1H), 7.19 (d,  $J$  = 8.8 Hz, 2H), 7.11 – 6.90 (m, 3H), 6.86 (d,  $J$  = 8.8 Hz, 1H), 3.90 (s, 3H), 3.64 (s, 2H), 3.16 (d,  $J$  = 5.8 Hz, 2H), 2.91 – 2.68 (m, 4H), 2.62 (t,  $J$  = 11.8 Hz, 2H), 2.24 – 1.98 (m, 2H), 1.81 (d,  $J$  = 13.6 Hz, 2H).  $^{13}C$  NMR (101 MHz,  $CDCl_3$ )  $\delta$  159.22 (dd,  $J_{C-F}$  = 140.6, 2.3 Hz), 156.81 (dd,  $J_{C-F}$  = 140.5, 2.3 Hz), 154.04, 140.95, 130.65, 127.81, 127.28 (dd,  $J_{C-F}$  = 17.0, 7.3 Hz), 117.38 (dd,  $J_{C-F}$  = 24.1, 4.9 Hz), 116.26 (dd,  $J_{C-F}$  = 25.2, 8.5 Hz), 114.99 (dd,  $J_{C-F}$  = 24.2, 8.5 Hz), 111.57, 111.45, 108.59, 100.61, 56.08, 55.32, 50.58, 48.84, 39.11, 36.43, 23.23. HRMS (ESI)  $m/z$  for  $C_{23}H_{26}F_2N_3O$  [M+H]. calcd 398.2044, found 398.2031.

**1-(3,5-Difluorobenzyl)-6'-methoxy-2',3',4',9'-tetrahydrospiro[piperidine-4,1'-pyrido[3,4-b]indole] (2c).**

Yield = 113 mg (57 %)  $^1H$  NMR (800 MHz,  $CDCl_3$ )  $\delta$  7.85 (s, 1H), 7.24 (d,  $J$  = 8.7 Hz, 1H), 7.00 – 6.92 (m, 3H), 6.84 (dd,  $J$  = 8.7, 2.4 Hz, 1H), 6.73 (tt,  $J$  = 8.9, 2.4 Hz, 1H), 3.88 (s, 3H), 3.58 (s, 2H), 3.16 (t,  $J$  = 5.7 Hz, 2H), 2.78 – 2.66 (m, 4H), 2.57 (td,  $J$  = 12.0, 2.4 Hz, 2H), 2.12 (td,  $J$  = 13.3, 4.3 Hz, 2H), 1.80 (dd,  $J$  = 14.1, 2.6 Hz, 2H).  $^{13}C$  NMR (201 MHz,  $CDCl_3$ )  $\delta$  163.66 (d,  $J_{C-F}$  = 12.9 Hz), 162.43 (d,  $J_{C-F}$  = 12.5 Hz), 154.08, 140.74, 130.55, 127.74, 111.52, 111.51 (dd,  $J_{C-F}$  = 20.9, 4.0 Hz), 111.49, 108.64, 102.48 (t,  $J_{C-F}$  = 25.5 Hz), 100.52, 62.34, 56.06, 50.54, 48.88, 39.09, 36.39, 23.21. HRMS (ESI)  $m/z$  for  $C_{23}H_{26}F_2N_3O$  [M+H]. calcd 398.2044, found 398.2030.



**6'-Methoxy-1-(3,4,5-trifluorobenzyl)-2',3',4',9'-tetrahydrospiro[piperidine-4,1'-pyrido[3,4-b]indole] (2d).**

Yield = 159 mg (77 %). <sup>1</sup>H NMR (400 MHz, CDCl<sub>3</sub>) δ 7.76 (s, 1H), 7.23 (d, *J* = 8.6 Hz, 1H), 7.04 (t, *J* = 7.5 Hz, 2H), 6.96 (d, *J* = 2.4 Hz, 1H), 6.84 (dt, *J* = 8.7, 1.8 Hz, 1H), 3.87 (s, 3H), 3.52 (s, 2H), 3.16 (t, *J* = 5.7 Hz, 2H), 2.71 (q, *J* = 5.3 Hz, 4H), 2.56 (t, *J* = 11.8 Hz, 2H), 2.10 (td, *J* = 13.2, 4.3 Hz, 2H), 1.81 (d, *J* = 13.7 Hz, 2H). <sup>13</sup>C NMR (201 MHz, CDCl<sub>3</sub>) δ 154.07, 151.14 (ddd, *J*<sub>C-F</sub> = 249.5, 10.1, 3.7 Hz), 140.68, 139.34 – 138.02 (m), 135.07, 130.58, 127.74, 112.54 (dd, *J*<sub>C-F</sub> = 17.1, 3.7 Hz), 111.53, 111.50, 108.64, 100.53, 61.90, 56.05, 50.55, 48.79, 39.08, 36.34, 23.19. HRMS (ESI) *m/z* for C<sub>23</sub>H<sub>24</sub>F<sub>3</sub>N<sub>3</sub>O [M+H]. calcd 416.1950, found 416.1939.

**6'-Methoxy-1-((perfluorophenyl)methyl)-2',3',4',9'-tetrahydrospiro[piperidine-4,1'-pyrido[3,4-b]indole] (2e).**

Yield = 202 mg (90 %). <sup>1</sup>H NMR (400 MHz, CDCl<sub>3</sub>) δ 7.73 (s, 1H), 7.19 (d, *J* = 8.7 Hz, 1H), 6.95 (t, *J* = 1.8 Hz, 1H), 6.83 (dt, *J* = 8.7, 1.9 Hz, 1H), 3.87 (d, *J* = 1.4 Hz, 3H), 3.79 (d, *J* = 2.4 Hz, 2H), 3.13 (t, *J* = 5.7 Hz, 2H), 2.76 (d, *J* = 11.1 Hz, 2H), 2.72 – 2.61 (m, 4H), 2.06 (td, *J* = 13.1, 4.5 Hz, 2H), 1.80 (d, *J* = 13.6 Hz, 2H). <sup>13</sup>C NMR (201 MHz, CDCl<sub>3</sub>) δ 154.03, 145.63 (d, *J*<sub>C-F</sub> = 248.0 Hz), 140.70, 140.59 (d, *J*<sub>C-F</sub> = 254.2 Hz), 137.39 (d, *J*<sub>C-F</sub> = 251.6 Hz), 130.54, 127.73, 111.47, 111.46, 110.75 (t, *J*<sub>C-F</sub> = 18.7 Hz), 108.66, 100.50, 56.01, 50.26, 48.92, 48.07, 39.04, 36.34, 23.20. HRMS (ESI) *m/z* for C<sub>23</sub>H<sub>23</sub>F<sub>5</sub>N<sub>3</sub>O [M+H]. calcd 452.1761, found 452.1753.

**1-(3,4-Difluorobenzyl)-6'-methoxy-2',3',4',9'-tetrahydrospiro[piperidine-4,1'-pyrido[3,4-b]indole] (2f).**

Yield = 88 mg (44 %). <sup>1</sup>H NMR (400 MHz, CDCl<sub>3</sub>) δ 8.15 – 7.91 (m, 1H), 7.25 (dt, *J* = 16.3, 7.7 Hz, 2H), 7.17 – 7.03 (m, 2H), 6.97 (s, 1H), 6.84 (dd, *J* = 8.8, 2.4 Hz, 1H), 3.88 (s, 3H), 3.55 (s, 2H), 3.16 (t, *J* = 5.7 Hz, 2H), 2.72 (q, *J* = 8.2, 6.0 Hz, 4H), 2.55 (t, *J* = 11.1 Hz, 2H), 2.11 (td, *J* = 13.5, 4.8 Hz, 2H), 1.81 (s, 2H). <sup>13</sup>C NMR (101 MHz, CDCl<sub>3</sub>) δ 154.05, δ 151.15 (dd, *J*<sub>C-F</sub> = 78.7, 12.7 Hz), 148.69 (dd, *J*<sub>C-F</sub> = 78.1, 12.5 Hz), 140.79, 135.47, 130.62, 127.76, 124.91, 117.80 (d, *J*<sub>C-F</sub> = 17.2 Hz), 116.90 (d, *J*<sub>C-F</sub> = 17.2 Hz), 111.52, 111.48, 108.59, 100.57, 62.14, 56.07, 50.62, 48.80, 39.10, 36.31, 23.21. HRMS (ESI) *m/z* for C<sub>23</sub>H<sub>26</sub>F<sub>2</sub>N<sub>3</sub>O [M+H]. calcd 398.2044, found 398.2032.

**6'-Methoxy-1-(2,3,4-trifluorobenzyl)-2',3',4',9'-tetrahydrospiro[piperidine-4,1'-pyrido[3,4-b]indole] (2g).**

Yield = 200 mg (96 %) <sup>1</sup>H NMR (400 MHz, CDCl<sub>3</sub>) δ 8.24 (s, 1H), 7.18 (d, *J* = 8.8 Hz, 1H), 7.15 – 7.03 (m, 1H), 6.99 – 6.86 (m, 2H), 6.85 – 6.67 (m, 1H), 3.87 (d, *J* = 2.9 Hz, 3H), 3.68 – 3.59 (m, 2H), 3.13 (t, *J* = 5.7 Hz, 2H), 2.77 – 2.65 (m, 4H), 2.65 – 2.50 (m, 2H), 2.16 – 1.98 (m, 2H), 1.85 – 1.71 (m, 2H). <sup>13</sup>C NMR (101 MHz, CDCl<sub>3</sub>) δ 153.99, 150.40 (ddd, *J*<sub>C-F</sub> = 250.2, 9.9, 2.6 Hz), 150.20 (d, *J*<sub>C-F</sub> = 250.4, 9.5, 3.0 Hz), 140.80, 139.88 (dt, *J*<sub>C-F</sub> = 251.8, 15.6 Hz), 130.65, 127.72, 124.92 (ddd, *J*<sub>C-F</sub> = 8.5, 6.3, 3.2 Hz), 122.42 (dd, *J*<sub>C-F</sub> = 12.1, 2.8 Hz), 111.71 (dd, *J*<sub>C-F</sub> = 17.1, 3.9 Hz), 111.51, 111.42, 108.52, 100.53, 56.05, 55.14, 50.49, 48.58, 39.08, 36.21, 23.20. HRMS (ESI) *m/z* for C<sub>23</sub>H<sub>24</sub>F<sub>3</sub>N<sub>3</sub>O [M+H]. calcd 416.1950, found 416.1941.

**1-(2,3-Difluorobenzyl)-6'-methoxy-2',3',4',9'-tetrahydrospiro[piperidine-4,1'-pyrido[3,4-b]indole] (2h).**

Yield = 184 mg (93 %) <sup>1</sup>H NMR (400 MHz, CDCl<sub>3</sub>) δ 7.85 (s, 1H), 7.20 (d, *J* = 8.8 Hz, 2H), 7.14 – 7.02 (m, 2H), 6.96 (d, *J* = 2.4 Hz, 1H), 6.83 (dd, *J* = 8.8, 2.4 Hz, 1H), 3.88 (s, 3H), 3.70 (d, *J* = 1.7 Hz, 2H), 3.15 (t, *J* = 5.7 Hz, 2H), 2.85 – 2.73 (m, 2H), 2.70 (t, *J* = 5.7 Hz, 2H), 2.60 (td, *J* = 11.9, 2.7 Hz, 2H), 2.16 – 1.99 (m, 2H), 1.80 (dq, *J* = 14.1, 2.9 Hz, 2H). <sup>13</sup>C NMR (101 MHz, CDCl<sub>3</sub>) δ 154.06, 151.26 (dd, *J*<sub>C-F</sub> = 119.9, 12.8 Hz), 148.79 (dd, *J*<sub>C-F</sub> = 119.9, 12.8 Hz), 140.86, 130.54, 127.77, 127.62 (d, *J*<sub>C-F</sub> = 11.4 Hz), 126.18 (t, *J*<sub>C-F</sub> = 3.5 Hz), 123.68 (dd, *J*<sub>C-F</sub> = 6.6, 4.8 Hz), 116.10, 115.93, 111.47, 108.62, 100.55, 56.06, 55.41, 50.52, 48.74, 39.10, 36.43, 23.21. HRMS (ESI) *m/z* for C<sub>23</sub>H<sub>26</sub>F<sub>2</sub>N<sub>3</sub>O [M+H]. calcd 398.2044, found 398.2037.

**6'-Methoxy-1-(2,4,5-trifluorobenzyl)-2',3',4',9'-tetrahydrospiro[piperidine-4,1'-pyrido[3,4-b]indole] (2i).**

Yield = 193 mg (93 %) <sup>1</sup>H NMR (400 MHz, CDCl<sub>3</sub>) δ 8.06 (s, 1H), 7.30 (ddd, *J* = 10.7, 8.9, 6.6 Hz, 1H), 7.19 (d, *J* = 8.6 Hz, 1H), 6.98 (d, *J* = 2.4 Hz, 1H), 6.95 – 6.86 (m, 1H), 6.84 (dd, *J* = 8.7, 2.5 Hz, 1H), 3.89 (s, 3H), 3.59 (d, *J* = 1.3 Hz, 2H), 3.16 (t, *J* = 5.7 Hz, 2H), 2.81 – 2.66 (m, 4H), 2.60 (dd, *J* = 23.9, 2.7 Hz, 2H), 2.10 (td, *J* = 13.7, 4.6 Hz, 2H), 1.80 (dd, *J* = 14.1, 2.7 Hz, 2H). <sup>13</sup>C NMR (101 MHz, CDCl<sub>3</sub>) δ 156.20 (ddd, *J*<sub>C-F</sub> = 247.5, 10.1, 2.2 Hz), 154.03, 149.1 (ddd, *J*<sub>C-F</sub> = 251.7, 14.9, 14.0), 146.8 (ddd, *J*<sub>C-F</sub> = 245.3, 12.5, 4.0), 140.79, 130.64, 127.76, 121.72 (dt, *J*<sub>C-F</sub> = 16.9, 4.6 Hz), 118.72 (dd, *J*<sub>C-F</sub> = 18.9, 5.7 Hz), 111.52, 111.47, 108.60, 105.31 (dd, *J*<sub>C-F</sub> = 28.6, 20.5 Hz), 100.57, 56.06, 54.76, 50.52, 48.70, 39.09, 36.34, 23.21. HRMS (ESI) *m/z* for C<sub>23</sub>H<sub>24</sub>F<sub>3</sub>N<sub>3</sub>O [M+H]. calcd 416.1950, found 416.1940.

**6'-Methoxy-2',3',4',9'-tetrahydrospiro[piperidine-4,1'-pyrido[3,4-b]indole] (3a).**

<sup>1</sup>H NMR (400 MHz, MeOD) δ 7.18 (d, *J* = 8.6 Hz, 1H), 6.90 (d, *J* = 2.4 Hz, 1H), 6.72 (dd, *J* = 8.7, 2.5 Hz, 1H), 3.80 (s, 3H), 3.11 – 2.94 (m, 4H), 2.84 (dt, *J* = 12.7, 3.9 Hz, 2H), 2.66 (t, *J* = 5.7 Hz, 2H), 1.96 (td, *J* = 13.5, 4.7 Hz, 2H), 1.72 (d, *J* = 12.8 Hz, 2H). <sup>13</sup>C NMR (101 MHz, MeOD) δ 153.53, 140.40, 131.32, 127.35, 110.98, 110.44, 106.88, 99.80, 54.91, 51.11, 40.53, 38.51, 35.15, 21.97. HRMS (ESI) *m/z* for C<sub>16</sub>H<sub>22</sub>N<sub>3</sub>O [M+H]. calcd 272.1763, found 272.1755.

**6'-Methoxy-1-(1-phenylethyl)-2',3',4',9'-tetrahydrospiro[piperidine-4,1'-pyrido[3,4-b]indole] (3b).**

Yield = 44 mg (36 %) <sup>1</sup>H NMR (800 MHz, MeOD) δ 7.45 – 7.42 (m, 2H), 7.39 (t, *J* = 7.7 Hz, 2H), 7.34 – 7.30 (m, 1H), 7.21 (d, *J* = 8.8 Hz, 1H), 6.92 (d, *J* = 2.4 Hz, 1H), 6.76 (dd, *J* = 8.7, 2.4 Hz, 1H), 3.81 (s, 3H), 3.21 (td, *J* = 6.0, 2.8 Hz, 2H), 3.18 – 3.15 (m, 1H), 2.82 (s, 1H), 2.80 – 2.76 (m, 2H), 2.65 (s, 1H), 2.56 (s, 1H), 2.32 (ddd, *J* = 14.4, 12.8, 4.5 Hz, 1H), 2.21 (ddd, *J* = 14.3, 12.9, 4.4 Hz, 1H), 2.05 (s, 1H), 1.99 – 1.94 (m, 1H), 1.85 (dd, *J* = 14.5, 2.9 Hz, 1H), 1.53 (d, *J* = 6.8 Hz, 3H). <sup>13</sup>C NMR (201 MHz, MeOD) δ 153.78, 137.50, 131.54, 128.28, 127.67, 127.45, 126.96, 116.74, 111.28, 111.16, 106.76, 99.71, 65.04, 54.85, 45.50, 45.38, 38.49, 34.03, 20.81, 18.26. HRMS (ESI) *m/z* for C<sub>24</sub>H<sub>30</sub>N<sub>3</sub>O [M+H]. calcd 376.2389, found 376.2389.

**6'-Methoxy-1-phenethyl-2',3',4',9'-tetrahydrospiro[piperidine-4,1'-pyrido[3,4-*b*]indole] (3c).**

Yield = 50 mg (40 %) <sup>1</sup>H NMR (800 MHz, MeOD) δ 7.32 (t, *J* = 7.5 Hz, 2H), 7.28 (d, *J* = 7.4 Hz, 2H), 7.24 – 7.11 (m, 2H), 6.92 (d, *J* = 2.5 Hz, 1H), 6.76 (dd, *J* = 8.7, 2.5 Hz, 1H), 3.81 (s, 3H), 3.17 (t, *J* = 5.8 Hz, 2H), 3.00 (d, *J* = 11.9 Hz, 2H), 2.92 (dd, *J* = 10.7, 6.0 Hz, 2H), 2.85 (dd, *J* = 10.8, 6.0 Hz, 2H), 2.80 – 2.61 (m, 4H), 2.20 (td, *J* = 13.8, 4.4 Hz, 2H), 1.89 (d, *J* = 14.1 Hz, 2H). <sup>13</sup>C NMR (201 MHz, MeOD) δ 153.67, 139.20, 138.53, 131.46, 128.34, 128.25, 127.17, 126.05, 111.18, 110.89, 107.14, 99.77, 59.60, 54.89, 51.27, 47.91, 38.56, 33.94, 32.27, 21.47. HRMS (ESI) *m/z* for C<sub>24</sub>H<sub>30</sub>N<sub>3</sub>O [M+H]. calcd 376.2389, found 376.2387.

**6'-Methoxy-1-(3-phenylpropyl)-2',3',4',9'-tetrahydrospiro[piperidine-4,1'-pyrido[3,4-*b*]indole] (3d).**

Yield = 21 mg (16 %) <sup>1</sup>H NMR (400 MHz, MeOD) δ 7.38 – 7.23 (m, 4H), 7.20 (dd, *J* = 8.3, 5.1 Hz, 2H), 6.97 – 6.86 (m, 1H), 6.75 (dt, *J* = 8.7, 1.7 Hz, 1H), 3.81 (s, 3H), 3.17 (t, *J* = 5.8 Hz, 2H), 3.01 (d, *J* = 12.0 Hz, 2H), 2.73 (dt, *J* = 14.8, 6.8 Hz, 8H), 2.21 (td, *J* = 13.9, 4.3 Hz, 2H), 2.06 – 1.85 (m, 4H). <sup>13</sup>C NMR (101 MHz, MeOD) δ 153.71, 141.28, 138.32, 131.47, 128.11, 128.06, 127.16, 125.72, 111.15, 110.95, 107.23, 99.74, 57.14, 54.87, 51.12, 47.93, 38.56, 33.74, 32.98, 27.41, 21.48. HRMS (ESI) *m/z* for C<sub>25</sub>H<sub>32</sub>N<sub>3</sub>O [M+H]. calcd 390.2545, found 390.2572.

**1-(Furan-2-ylmethyl)-6'-methoxy-2',3',4',9'-tetrahydrospiro[piperidine-4,1'-pyrido[3,4-*b*]indole] (3e).**

Yield = 23 mg (18 %) <sup>1</sup>H NMR (400 MHz, CDCl<sub>3</sub>) δ 8.13 (s, 1H), 7.41 (s, 1H), 7.20 (dd, *J* = 8.8, 1.3 Hz, 1H), 6.92 (t, *J* = 1.8 Hz, 1H), 6.80 (dt, *J* = 8.7, 1.9 Hz, 1H), 6.37 – 6.30 (m, 2H), 3.84 (d, *J* = 1.4 Hz, 3H), 3.70 (s, 2H), 3.11 (t, *J* = 5.7 Hz, 2H), 2.84 (d, *J* = 11.6 Hz, 2H), 2.71 – 2.64 (m, 4H), 2.24 (td, *J* = 13.5, 4.2 Hz, 2H), 1.80 (d, *J* = 13.8 Hz, 2H). <sup>13</sup>C NMR (101 MHz, CDCl<sub>3</sub>) δ 154.13, 150.38, 142.80, 140.42, 130.74, 127.70, 111.74, 111.62, 110.48, 110.06, 108.63, 100.60, 56.17, 54.84, 50.47, 48.66, 39.29, 35.91, 23.33. HRMS (ESI) *m/z* for C<sub>21</sub>H<sub>26</sub>N<sub>3</sub>O<sub>2</sub> [M+H]. calcd 352.2025, found 352.2024.

**6'-Methoxy-1-(pyridin-2-ylmethyl)-2',3',4',9'-tetrahydrospiro[piperidine-4,1'-pyrido[3,4-*b*]indole] (3f).**

Yield = 118 mg (65 %) <sup>1</sup>H NMR (400 MHz, CDCl<sub>3</sub>) δ 8.59 (d, *J* = 4.9 Hz, 1H), 8.34 (s, 1H), 7.63 (t, *J* = 7.7 Hz, 1H), 7.41 (d, *J* = 7.8 Hz, 1H), 7.17 (d, *J* = 8.3 Hz, 2H), 6.93 (s, 1H), 6.78 (dd, *J* = 8.7, 2.6 Hz, 1H), 3.84 (s, 3H), 3.76 (s, 2H), 3.12 (t, *J* = 5.7 Hz, 2H), 2.77 (d, *J* = 11.4 Hz, 2H), 2.71 – 2.58 (m, 4H), 2.15 (td, *J* = 13.4, 12.8, 4.3 Hz, 2H), 1.75 (d, *J* = 13.6 Hz, 2H). <sup>13</sup>C NMR (101 MHz, CDCl<sub>3</sub>) δ 158.30, 153.99, 149.46, 140.95, 136.54, 130.73, 127.70, 123.53, 122.28, 111.65, 111.37, 108.38, 100.51, 64.61, 56.10, 50.63, 49.14, 39.18, 36.19, 23.26. HRMS (ESI) *m/z* for C<sub>22</sub>H<sub>27</sub>N<sub>4</sub>O [M+H]. calcd 363.2185, found 363.2188.

**6'-Methoxy-1-(pyridin-3-ylmethyl)-2',3',4',9'-tetrahydrospiro[piperidine-4,1'-pyrido[3,4-*b*]indole] (3g).**

Yield = 61 mg (34 %) <sup>1</sup>H NMR (400 MHz, MeOD) δ 8.53 (s, 1H), 8.44 (d, *J* = 4.9 Hz, 1H), 7.80 (dd, *J* = 7.8, 2.2 Hz, 1H), 7.39 (dd, *J* = 7.9, 5.0 Hz, 1H), 7.15 (d, *J* = 8.9 Hz, 1H), 6.88

(d,  $J = 2.3$  Hz, 1H), 6.70 (dt,  $J = 8.8, 1.8$  Hz, 1H), 3.78 (s, 3H), 3.58 (s, 2H), 3.02 (t,  $J = 5.7$  Hz, 2H), 2.64 (t,  $J = 5.6$  Hz, 4H), 2.46 (t,  $J = 12.1$  Hz, 2H), 2.06 (tt,  $J = 14.1, 7.0$  Hz, 2H), 1.69 (d,  $J = 13.7$  Hz, 2H).  $^{13}\text{C}$  NMR (101 MHz, MeOD)  $\delta$  153.55, 149.62, 147.56, 139.80, 137.96, 134.14, 131.35, 127.32, 123.72, 111.09, 110.52, 107.03, 99.77, 59.46, 54.91, 50.90, 48.08, 38.43, 34.75, 21.82. HRMS (ESI)  $m/z$  for  $\text{C}_{22}\text{H}_{27}\text{N}_4\text{O}$  [M+H]. calcd 363.2185, found 363.2180.

**1-(4-(*tert*-Butyl)benzyl)-6'-methoxy-2',3',4',9'-tetrahydrospiro[piperidine-4,1'-pyrido[3,4-*b*]indole] (3h).**

Yield = 111 mg (53 %).  $^1\text{H}$  NMR (400 MHz,  $\text{CDCl}_3$ )  $\delta$  8.52 (br, 1H), 7.32 (s, 4H), 7.22 (d,  $J = 8.8$  Hz, 1H), 6.97 (d,  $J = 2.4$  Hz, 1H), 6.82 (dd,  $J = 8.8, 2.6$  Hz, 1H), 3.88 (s, 3H), 3.63 (s, 2H), 3.15 (t,  $J = 5.7$  Hz, 2H), 2.82 (d,  $J = 11.6$  Hz, 2H), 2.71 (t,  $J = 5.7$  Hz, 2H), 2.57 (td,  $J = 12.1, 2.4$  Hz, 2H), 2.20 (td,  $J = 13.4, 4.4$  Hz, 2H), 1.79 (s, 2H), 1.34 (s, 9H).  $^{13}\text{C}$  NMR (101 MHz,  $\text{CDCl}_3$ )  $\delta$  153.97, 150.32, 140.87, 134.19, 130.71, 129.29, 127.67, 125.27, 111.58, 111.39, 108.34, 100.53, 62.95, 56.09, 50.63, 48.87, 39.17, 36.03, 34.51, 31.40, 23.27. HRMS (ESI)  $m/z$  for  $\text{C}_{27}\text{H}_{36}\text{N}_3\text{O}$  [M+H]. calcd 418.2858, found 418.2849.

**1-(2,4-Difluorobenzyl)-6'-methoxy-2',3',4',9'-tetrahydrospiro[azepane-4,1'-pyrido[3,4-*b*]indole] (4a).**

Yield = 56 mg (76 %)  $^1\text{H}$  NMR (400 MHz, MeOD)  $\delta$  7.48 – 7.31 (m, 1H), 7.23 (d,  $J = 8.7$  Hz, 1H), 7.09 – 6.92 (m, 2H), 6.91 (t,  $J = 1.8$  Hz, 1H), 6.75 (dt,  $J = 8.9, 1.9$  Hz, 1H), 3.79 (s, 3H), 3.67 (s, 2H), 3.15 (dp,  $J = 24.7, 6.3, 5.8$  Hz, 2H), 2.75 (h,  $J = 6.8$  Hz, 6H), 2.09 (dtd,  $J = 44.9, 14.8, 7.3$  Hz, 3H), 1.86 (dd,  $J = 13.8, 6.4$  Hz, 1H), 1.72 (p,  $J = 5.9$  Hz, 2H).  $^{13}\text{C}$  NMR (101 MHz, MeOD)  $\delta$  163.37 (dd,  $J_{\text{C-F}} = 93.9, 12.1$  Hz), 160.91 (dd,  $J_{\text{C-F}} = 94.0, 12.2$  Hz), 153.70, 138.27, 132.81 (dd,  $J_{\text{C-F}} = 9.7, 6.1$  Hz), 131.21, 127.05, 121.39 (dd,  $J_{\text{C-F}} = 14.6, 3.7$  Hz), 111.36, 110.90 (dd,  $J_{\text{C-F}} = 21.2, 3.7$  Hz), 110.89, 105.10, 103.44 (t,  $J_{\text{C-F}} = 26.0$  Hz), 99.84, 57.47, 55.62, 54.89, 53.95, 50.44, 38.60, 38.56, 36.75, 24.83, 20.59. HRMS (ESI)  $m/z$  for  $\text{C}_{24}\text{H}_{28}\text{F}_2\text{N}_3\text{O}$  [M+H]. calcd 412.2200, found 412.2193.

**1'-(2,4-Difluorobenzyl)-6-methoxy-2,3,4,9-tetrahydrospiro[pyrido[3,4-*b*]indole-1,3'-pyrrolidine] (4b).**

Yield = 83 mg (43 %)  $^1\text{H}$  NMR (800 MHz,  $\text{CDCl}_3$ )  $\delta$  8.87 (s, 1H), 7.33 (td,  $J = 8.6, 6.6$  Hz, 1H), 7.24 (d,  $J = 8.7$  Hz, 1H), 6.94 (d,  $J = 2.6$  Hz, 1H), 6.89 – 6.84 (m, 2H), 6.83 (dd,  $J = 8.7, 2.6$  Hz, 1H), 3.87 (s, 3H), 3.79 – 3.73 (m, 2H), 3.26 (dt,  $J = 13.0, 4.6$  Hz, 1H), 3.18 – 3.07 (m, 3H), 2.78 – 2.68 (m, 2H), 2.64 (q,  $J = 9.0$  Hz, 1H), 2.53 (d,  $J = 8.9$  Hz, 1H), 2.34 (dt,  $J = 13.3, 8.5$  Hz, 1H), 2.14 (ddd,  $J = 13.0, 9.2, 3.1$  Hz, 1H).  $^{13}\text{C}$  NMR (201 MHz,  $\text{CDCl}_3$ )  $\delta$  162.58 (dd,  $J_{\text{C-F}} = 208.3, 11.7$  Hz), 161.34 (dd,  $J_{\text{C-F}} = 208.7, 12.1$  Hz), 153.96, 140.73, 132.11–132.03 (m), 130.58, 127.26, 120.86, 111.63, 111.30, 111.21 (dd,  $J_{\text{C-F}} = 21.3, 3.7$  Hz), 106.03, 104.09 (t,  $J_{\text{C-F}} = 25.7$  Hz), 100.49, 65.57, 59.95, 56.05, 52.59, 52.48, 41.80, 39.15, 22.30. HRMS (ESI)  $m/z$  for  $\text{C}_{22}\text{H}_{24}\text{F}_2\text{N}_3\text{O}$  [M+H]. calcd 384.1887, found 384.1894.

**1-(2,4-Difluorobenzyl)-6'-methoxy-2',3',4',9'-tetrahydrospiro[piperidine-3,1'-pyrido[3,4-b]indole] (4c).**

Yield = 85 mg (43 %) <sup>1</sup>H NMR (400 MHz, CDCl<sub>3</sub>) δ 9.65 (s, 1H), 7.31 – 7.27 (m, 1H), 7.22 (d, *J* = 6.7 Hz, 1H), 6.96 (d, *J* = 2.2 Hz, 1H), 6.90 – 6.76 (m, 3H), 3.88 (s, 3H), 3.60 (q, *J* = 12.9 Hz, 2H), 3.47 – 3.17 (m, 2H), 3.00 (s, 1H), 2.92 – 2.61 (m, 3H), 2.43 – 2.05 (m, 3H), 1.96 – 1.67 (m, 2H), 1.58 (s, 1H). <sup>13</sup>C NMR (101 MHz, CDCl<sub>3</sub>) δ 163.37 (dd, *J*<sub>C-F</sub> = 84.4, 12.1 Hz), 160.90 (dd, *J*<sub>C-F</sub> = 84.5, 12.3 Hz), 153.79, 139.99, 132.55 (dd, *J*<sub>C-F</sub> = 9.5, 6.2 Hz), 130.43, 127.18, 120.51 (dd, *J*<sub>C-F</sub> = 14.3, 3.7 Hz), 111.74, 111.31, 111.13 (dd, *J*<sub>C-F</sub> = 20.9, 3.7 Hz), 106.14, 104.29 (t, *J*<sub>C-F</sub> = 25.9 Hz), 100.22, 63.38, 56.48, 56.07, 53.34, 52.17, 38.90, 36.31, 22.64, 22.09. HRMS (ESI) *m/z* for C<sub>23</sub>H<sub>26</sub>F<sub>2</sub>N<sub>3</sub>O [M+H]. calcd 398.2044, found 398.2040.

**1-Benzyl-N-(2-(5-methoxy-1*H*-indol-3-yl)ethyl)piperidin-4-amine (4d).**

Yield = 105 mg (53 %) <sup>1</sup>H NMR (400 MHz, CDCl<sub>3</sub>) δ 8.37 (s, 1H), 7.34 (q, *J* = 7.8 Hz, 1H), 7.30 – 7.18 (m, 1H), 7.01 (s, 1H), 6.83 (dt, *J* = 32.9, 9.1 Hz, 3H), 3.88 (s, 3H), 3.53 (s, 2H), 2.98 (dq, *J* = 11.1, 6.8 Hz, 4H), 2.84 (d, *J* = 11.2 Hz, 2H), 2.50 (tt, *J* = 10.0, 4.3 Hz, 1H), 2.07 (t, *J* = 11.5 Hz, 2H), 1.86 (d, *J* = 12.4 Hz, 2H), 1.54 – 1.24 (m, 2H). <sup>13</sup>C NMR (101 MHz, CDCl<sub>3</sub>) δ 162.87 (dd, *J*<sub>C-F</sub> = 77.0, 12.3 Hz), 160.41 (dd, *J*<sub>C-F</sub> = 78.0, 11.8 Hz), 153.88, 132.19 (dd, *J*<sub>C-F</sub> = 9.5, 6.2 Hz), 131.61, 127.85, 122.84, 120.95 (dd, *J*<sub>C-F</sub> = 15.0, 3.7 Hz), 113.56, 112.16, 111.91, 110.96 (dd, *J*<sub>C-F</sub> = 20.9, 3.7 Hz), 103.48 (t, *J*<sub>C-F</sub> = 25.7 Hz), 100.75, 55.97, 54.82, 54.65, 52.15, 46.76, 32.66, 26.02. HRMS (ESI) *m/z* for C<sub>23</sub>H<sub>28</sub>F<sub>2</sub>N<sub>3</sub>O [M+H]. calcd 400.2200, found 400.2188.

**1-(2,4-Difluorobenzyl)-2',3',4',9'-tetrahydrospiro[piperidine-4,1'-pyrido[3,4-b]indole] (5a).**

Yield = 103 mg (56 %) <sup>1</sup>H NMR (400 MHz, CDCl<sub>3</sub>) δ 8.94 (s, 1H), 7.51 (d, *J* = 7.5 Hz, 1H), 7.43 – 7.25 (m, 2H), 7.13 (hept, *J* = 8.4, 7.5 Hz, 2H), 6.84 – 6.61 (m, 2H), 3.66 (s, 2H), 3.13 (t, *J* = 5.7 Hz, 2H), 2.86 – 2.69 (m, 4H), 2.69 – 2.52 (m, 2H), 2.19 (dt, *J* = 13.0, 7.5 Hz, 2H), 1.73 (d, *J* = 13.7 Hz, 2H). <sup>13</sup>C NMR (101 MHz, CDCl<sub>3</sub>) δ 163.22 (dd, *J*<sub>C-F</sub> = 91.1, 11.9 Hz), 160.74 (dd, *J*<sub>C-F</sub> = 91.6, 11.9 Hz), 139.72, 135.68, 132.93 (dd, *J*<sub>C-F</sub> = 9.5, 5.9 Hz), 127.30, 121.56, 119.77 (dd, *J*<sub>C-F</sub> = 15.0, 3.7 Hz), 119.18, 118.12, 111.21 (dd, *J*<sub>C-F</sub> = 21.3, 3.7 Hz), 110.99, 108.50, 103.78 (t, *J*<sub>C-F</sub> = 25.7 Hz), 55.07, 50.44, 48.50, 39.14, 35.77, 23.15. HRMS (ESI) *m/z* for C<sub>22</sub>H<sub>24</sub>F<sub>2</sub>N<sub>3</sub> [M+H]. calcd 368.1938, found 368.1935.

**6'-Bromo-1-(2,4-difluorobenzyl)-2',3',4',9'-tetrahydrospiro[piperidine-4,1'-pyrido[3,4-b]indole] (5b).**

Yield = 51 mg (54 %) <sup>1</sup>H NMR (400 MHz, CDCl<sub>3</sub>) δ 8.83 (s, 1H), 7.60 (d, *J* = 2.1 Hz, 1H), 7.36 (td, *J* = 8.7, 6.6 Hz, 1H), 7.19 (dd, *J* = 8.6, 2.0 Hz, 1H), 7.12 (d, *J* = 8.5 Hz, 1H), 6.83 – 6.68 (m, 2H), 3.65 (s, 2H), 3.11 (t, *J* = 5.7 Hz, 2H), 2.77 (dd, *J* = 8.4, 2.9 Hz, 2H), 2.70 – 2.57 (m, 4H), 2.14 (td, *J* = 13.3, 4.6 Hz, 2H), 1.72 (dd, *J* = 14.1, 2.4 Hz, 2H). <sup>13</sup>C NMR (101 MHz, CDCl<sub>3</sub>) δ 163.19 (dd, *J*<sub>C-F</sub> = 93.7, 11.9 Hz), 160.72 (dd, *J*<sub>C-F</sub> = 94.1, 11.9 Hz), 141.14, 134.23, 132.81 (dd, *J*<sub>C-F</sub> = 9.7, 5.7 Hz), 129.14, 124.23, 120.79, 119.76 (dd, *J*<sub>C-F</sub> = 14.9, 3.9 Hz), 112.38, 112.31, 111.19 (dd, *J*<sub>C-F</sub> = 21.1, 3.9 Hz), 108.39, 103.80 (t, *J*<sub>C-F</sub> = 25.9 Hz), 55.12, 50.39, 48.46, 38.99, 35.76, 22.99. HRMS (ESI) *m/z* for C<sub>22</sub>H<sub>23</sub>BrF<sub>2</sub>N<sub>3</sub> [M+H]. calcd 446.1043, found 446.1036.

**6'-Chloro-1-(2,4-difluorobenzyl)-2',3',4',9'-tetrahydrospiro[piperidine-4,1'-pyrido[3,4-b]indole] (5c).**

Yield = 134 mg (67 %). <sup>1</sup>H NMR (400 MHz, CDCl<sub>3</sub>) δ 8.86 – 8.49 (m, 1H), 7.43 (d, *J* = 9.3 Hz, 2H), 7.21 (d, *J* = 8.7 Hz, 1H), 7.08 (d, *J* = 8.5 Hz, 1H), 6.82 (q, *J* = 9.0 Hz, 2H), 3.69 (s, 2H), 3.11 (d, *J* = 5.8 Hz, 2H), 2.81 (d, *J* = 11.3 Hz, 2H), 2.67 (q, *J* = 8.5, 8.0 Hz, 4H), 2.18 (q, *J* = 8.0, 5.3 Hz, 2H), 1.76 (d, *J* = 13.6 Hz, 2H). <sup>13</sup>C NMR (101 MHz, CDCl<sub>3</sub>) δ 163.25 (dd, *J*<sub>C-F</sub> = 100.2, 12.4 Hz), 160.77 (dd, *J*<sub>C-F</sub> = 100.6, 12.3 Hz), 141.11, 133.91, 132.90 (dd, *J*<sub>C-F</sub> = 9.8, 5.8 Hz), 128.44, 124.90, 121.74, 119.48 (d, *J*<sub>C-F</sub> = 15.4 Hz), 117.69, 111.85, 111.29 (d, *J*<sub>C-F</sub> = 20.7 Hz), 108.51, 103.82 (t, *J*<sub>C-F</sub> = 25.7 Hz), 54.96, 50.36, 48.43, 39.00, 35.72, 22.99. HRMS (ESI) *m/z* for C<sub>22</sub>H<sub>23</sub>ClF<sub>2</sub>N<sub>3</sub> [M+H]. calcd 402.1549, found 402.1539.

**1-(2,4-Difluorobenzyl)-7'-methoxy-2',3',4',9'-tetrahydrospiro[piperidine-4,1'-pyrido[3,4-b]indole] (5d).**

Yield = 90 mg (45 %). <sup>1</sup>H NMR (400 MHz, CDCl<sub>3</sub>) δ 8.24 (s, 1H), 7.48 – 7.32 (m, 2H), 6.94 – 6.68 (m, 4H), 3.82 (s, 3H), 3.67 (s, 2H), 3.13 (t, *J* = 5.7 Hz, 2H), 2.83 – 2.76 (m, 2H), 2.72 – 2.54 (m, 4H), 2.17 (td, *J* = 13.5, 13.1, 4.4 Hz, 2H), 1.77 (d, *J* = 13.7 Hz, 2H). <sup>13</sup>C NMR (101 MHz, CDCl<sub>3</sub>) δ 163.17 (dd, *J*<sub>C-F</sub> = 91.6, 11.9 Hz), 160.70 (dd, *J*<sub>C-F</sub> = 92.1, 12.1 Hz), 156.28, 138.34, 136.25, 132.75 (dd, *J*<sub>C-F</sub> = 9.5, 5.9 Hz), 121.77, 119.96 (dd, *J*<sub>C-F</sub> = 14.8, 3.8 Hz), 118.65, 111.20 (dd, *J*<sub>C-F</sub> = 20.8, 3.8 Hz), 108.93, 108.49, 103.74 (t, *J*<sub>C-F</sub> = 25.7 Hz), 94.99, 55.78, 54.99, 50.38, 48.59, 39.15, 35.97, 23.14. HRMS (ESI) *m/z* for C<sub>23</sub>H<sub>26</sub>F<sub>2</sub>N<sub>3</sub>O [M+H]. calcd 398.2044, found 398.2033.

**1-(2,4-Difluorobenzyl)-6'-methoxy-9'-methyl-2',3',4',9'-tetrahydrospiro[piperidine-4,1'-pyrido[3,4-b]indole] (5e).**

Yield = 47 mg (23 %). <sup>1</sup>H NMR (400 MHz, CDCl<sub>3</sub>) δ 7.45 (q, *J* = 8.1 Hz, 1H), 7.20 (d, *J* = 8.7 Hz, 1H), 6.97 (d, *J* = 2.4 Hz, 1H), 6.87 (dtd, *J* = 28.7, 9.4, 2.5 Hz, 3H), 3.89 (s, 6H), 3.65 (s, 2H), 3.10 (t, *J* = 5.7 Hz, 2H), 2.72 (tt, *J* = 18.0, 9.9 Hz, 6H), 2.52 – 2.22 (m, 2H), 1.72 (d, *J* = 13.7 Hz, 2H). <sup>13</sup>C NMR (101 MHz, CDCl<sub>3</sub>) δ 162.63 (d, *J*<sub>C-F</sub> = 11.9 Hz), 160.15 (d, *J*<sub>C-F</sub> = 12.1 Hz), 153.93, 140.67, 132.74, 132.27 (br), 126.69, 120.93 (br), 111.39, 111.02 (d, *J*<sub>C-F</sub> = 21.6 Hz), 109.59, 109.17, 103.62 (t, *J*<sub>C-F</sub> = 25.7 Hz), 100.23, 56.10, 54.96, 51.63, 48.56, 38.81, 34.79, 32.32, 24.10. HRMS (ESI) *m/z* for C<sub>24</sub>H<sub>28</sub>F<sub>3</sub>N<sub>3</sub>O [M+H]. calcd 412.2200, found 412.2191.

**(+/-)-(2*R*,11*aS*)-6'-methoxy-1,2',3,3',4,4',6,9',11,11*a*-decahydrospiro[pyrido[1,2-*b*]isoquinoline-2,1'-pyrido[3,4-*b*]indole] (6b).**

<sup>1</sup>H NMR (599 MHz, cdcl<sub>3</sub>) δ 8.34 (d, *J* = 20.8 Hz, 1H), 7.14 (dq, *J* = 13.2, 6.7, 6.2 Hz, 2H), 7.11 – 6.99 (m, 3H), 6.94 (d, *J* = 2.6 Hz, 1H), 6.78 (dt, *J* = 8.7, 2.3 Hz, 1H), 3.86 (s, 4H), 3.52 (d, *J* = 15.3 Hz, 1H), 3.22 – 3.08 (m, 2H), 2.94 – 2.88 (m, 1H), 2.84 (tq, *J* = 8.2, 3.1, 2.6 Hz, 1H), 2.77 – 2.72 (m, 3H), 2.69 (t, *J* = 5.7 Hz, 2H), 2.29 – 2.19 (m, 1H), 2.00 (dt, *J* = 13.9, 3.1 Hz, 1H), 1.92 – 1.82 (m, 2H). <sup>13</sup>C NMR (101 MHz, CDCl<sub>3</sub>) δ 153.98, 140.49, 133.80, 133.42, 130.74, 128.10, 127.67, 126.40, 126.02, 125.81, 111.62, 111.46, 108.47, 100.46, 57.58, 56.05, 52.91, 51.35, 50.40, 43.76, 39.28, 36.37, 35.64, 23.26. HRMS (ESI) *m/z* for C<sub>24</sub>H<sub>28</sub>N<sub>3</sub>O [M+H]. calcd 374.2232, found 374.2222.



## Supplementary Material

Refer to Web version on PubMed Central for supplementary material.

## ACKNOWLEDGEMENTS:

This work was supported by the Cystic Fibrosis Foundation [HAGGIE19R2 and HAGGIE20XX0]; the National Institutes of Health [DK072517, DK099803, DK075302, EY13574]; and the UC Davis Tara K. Telford CF Fund [fellowship to J.S.Z.]. The authors thank Dr. Christine Bear (Hospital for Sick Children, Toronto, Canada) for provision of the gene edited 16HBE14o- cells expressing I1234del-CFTR, Drs. Martin Mense and Hillary Valley (Cystic Fibrosis Foundation Therapeutics Laboratory) for provision of the gene edited 16HBE14o-cells expressing N1303K-CFTR, and Drs. Andras Rab and Jeong Hong (Emory University) for provision of the FRT cell model expressing R347P-CFTR. The authors also thank Dr. Marc Anderson (San Francisco State University) for helpful discussions.

## ABBREVIATIONS USED:

<b>CFTR</b>	cystic fibrosis transmembrane conductance regulator
<b>DMF</b>	dimethylformamide
<b>DMSO</b>	dimethyl sulfoxide
<b>FRT</b>	Fischer Rat Thyroid
<b>HPLC</b>	high-performance liquid chromatography
<b>HRMS</b>	high-resolution mass spectrometry
<b>MAD</b>	mean absolute deviation
<b>MMFF</b>	Merck Molecular Force Field
<b>PBS</b>	phosphate-buffered saline
<b>PTCs</b>	premature termination codons
<b>RT</b>	room temperature
<b>TLC</b>	thin layer chromatography

## REFERENCES

1. Elborn JS (2016) Cystic Fibrosis. *Lancet* 388:2519–2531. [PubMed: 27140670]
2. Keating D, Marigowda G, Burr L, Daines C, Mall MA, McKone EF, Ramsey BW, Rowe SM, Sass LA, Tullis E, McKee CM, Moskowitz SM, Robertson S, Savage J, Simard C, Van Goor F, Waltz D, Xuan F, Young T, Taylor-Cousar and JL VX16-445-001 Study Group (2018) VX-445-Tezacaftor-Ivacaftor in patients with cystic fibrosis and one or two Phe508del alleles. *N. Engl. J. Med* 379:1612–1620. [PubMed: 30334692]
3. Heijerman HGM, McKone EF, Downey DG, Van Braeckel E, Rowe SM, Tullis E, Mall MA, Welter JJ, Ramsey BW, McKee CM, Marigowda G, Moskowitz SM, Waltz D, Sosnay PR, Simard C, Ahluwalia N, Xuan F, Zhang Y, Taylor-Cousar JL, McCoy and KS V17-445-103 Trial Group (2019) Efficacy and safety of the elexacaftor plus tezacaftor plus ivacaftor combination regimen in people with cystic fibrosis homozygous for the F508del mutation: a double-blind, randomized, phase 3 trial. *Lancet* 394:1940–1948. [PubMed: 31679946]



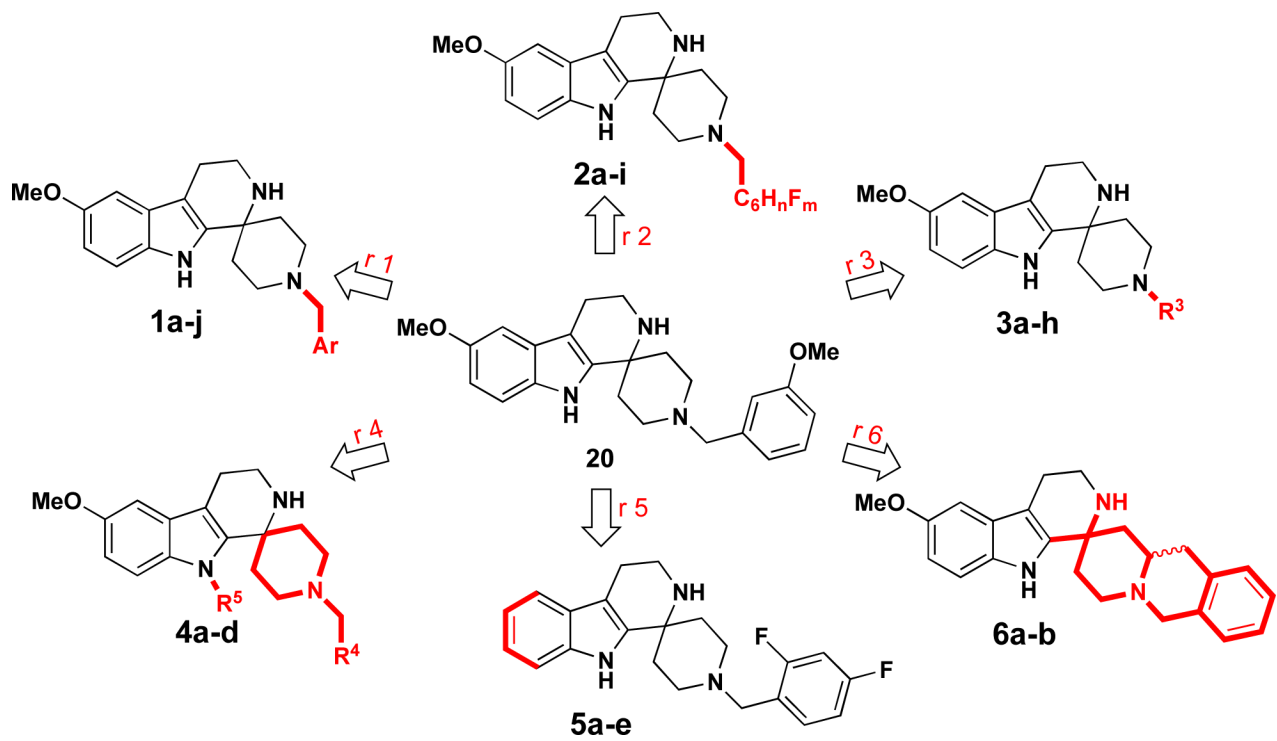
4. Middleton PG, Mall MA, Drevinek P, Lands LC, McKone EF, Polineni D, Ramsey BW, Taylor-Cousar JL, Tullis E, Vermeulen F, Marigowda G, McKee CM, Moskowitz SM, Nair N, Savage J, Simard C, Tian F, Waltz D, Xuan F, Rowe SM, Jain and R V17-445-102 Study Group (2019) Elexacaftor-tezacaftor-ivacaftor for cystic fibrosis with a single Phe508del allele. *N. Engl. J. Med* 381:1809–1819. [PubMed: 31697873]
5. Burgener EB and Moss RB (2018) Cystic fibrosis transmembrane conductance regulator modulators: precision medicine in cystic fibrosis. *Curr. Opin. Pediatr* 30:372–377. [PubMed: 29538046]
6. Kym PR, Wang X, Pizzonero M and Van der Plas SE (2018) Recent progress in the discovery and development of small-molecule modulators of CFTR. *Prog. Med. Chem* 57:235–276. [PubMed: 29680149]
7. Haggie PM, Phuan P-W, Tan JA, Xu H, Avramescu RG, Perdomo D, Zlock L, Nielson DW, Finkbeiner WE, Lukacs GL and Verkman AS (2017) Correctors and potentiators rescue function of the truncated W1282X-cystic fibrosis transmembrane regulator (CFTR) translation product. *J. Biol. Chem* 292:771–785. [PubMed: 27895116]
8. Phuan P-W, Son J-H, Tan JA, Li C, Musante I, Zlock L, Nielson DW, Finkbeiner WE, Kurth MJ, Galiotta LJ, Haggie PM and Verkman AS (2018) Combination potentiator ('co-potentiator') therapy for CF caused by CFTR mutants, including N1303K, that are poorly responsive to single potentiators. *J. Cyst. Fibros* 17:595–606. [PubMed: 29903467]
9. Phuan P-W, Tan JA, Rivera AA, Zlock L, Nielson D, Finkbeiner WE, Haggie PM and Verkman AS (2019) Nanomolar-potency 'co-potentiators' for therapy of a defined subset of minimal function CFTR mutations. *Sci. Rep* 9:17640. [PubMed: 31776420]
10. Mokrosz MJ, Bartyzel P and Mokorosz JL (1993) Structure and spectral properties of b-carbolines. 5. Synthesis and stereochemistry of new trihydrodiazabicyclo[3.m.n]alkano[4',5':1,2]-pyrido[3,4-b]-indole ring systems. *J. Hetero. Chem* 30:1543–1548.
11. Bridges TM, Brady AE, Kennedy JP, Daniels RN, Miller NR, Kim K, Breininger ML, Gentry PR, Brogan JT, Jones CK, Conn PJ and Lindsley CW (2008) Synthesis and SAR of analogues of the M1 allosteric agonist TBPB. Part I: Exploration of alternative benzyl and privileged structure moieties. *Bioorg. Med. Chem. Lett* 18:5439–5442. [PubMed: 18805692]
12. Abd Rabo M, Mahmoud M and Pagenkopf BL (2010) Synthesis of 5-azaindoles via a cycloaddition reaction between nitriles and donor-acceptor cyclopropanes. *Org. Letts* 12:3168–3171. [PubMed: 20550103]
13. Pictet A and Spengler T (1911) Über die bildung von isochinolin-derivaten durch einwirkung von methylal auf phenyl-athylamin, phenyl-alanin und tyrosin. *Berichte der Deutschen Chemischen Gesellschaft* 44:2030–2036.
14. Cox ED and Cook JM (1995) The Pictet-Spengler condensation: a new direction for an old reaction. *Chem. Rev* 95:1797–1842.
15. Buchi G and Mak C-P (1977) Nitro olefination of indoles and some substituted benzenes with 1-dimethylamino-2-nitroethylene. *J. Org. Chem* 42:1784–1786.
16. Ranjan P, Ojeda GM, Sharma UK and Van der Eycken EV (2019) Metal-free dearomatization: Direct access to spiroindol(en)ines in batch and continuous-flow. *Chem. Eur. J* 25:2442–2446. [PubMed: 30507048]
17. Becke AD (1993) Density-functional thermochemistry. III. The role of exact exchange. *J. Phys. Chem* 98:5648–5652.
18. Lee CJ, Wang W and Parr RG (1988) Development of Colle-Selvatti correlation-energy formula into a function of the electron density. *Phys. Rev. B: Condens. Matter Mater. Phys* 37:785–789.
19. Miehlich B, Savin A, Stoll H and Preuss H (1989) Results obtained with the correlation energy density functionals of Becke and Lee, Yang and Parr. *Chem. Phys. Lett* 157:200–206.
20. Cammi R, Mennucci B and Tomasi J, In computational chemistry; Reviews of current trends, in *In computational chemistry; Reviews of current trends.*, Leszczynski J, Editor. 2003, World Scientific Publishing Co. Pte. Ltd.: Singapore.
21. Grimme S, Antony J, Ehrlich S and Krieg H (2010) A consistent and accurate ab initio parameterization of density functional dispersion correction (DFT-D) for the 94 elements H-Pu. *J. Chem. Phys* 132:154104. [PubMed: 20423165]

22. Grimme S, Ehrlich S and Goerigk L (2011) Effect of damping function in dispersion corrected density functional theory. *J. Comp. Chem* 132:1456.
23. Lee JK and Tantillo DJ (2003) Computational insights into the mechanism of orotidine monophosphate decarboxylase. *Adv. Phys. Org. Chem* 38:183–218.
24. Jursic BS (1996) Computation of electronic affinities of O and F atoms, and energy profile of F-H2 reaction by density functional theory. *J. Chem. Phys* 104:4151.
25. Humphrey W, Dalke A and Schulten K (1996) VMD - Visual Molecular Dynamics. *J. Mol. Graphics* 14:33–38.
26. Sharp K and Matschinsky F (2015) Translation of Ludwig Boltzmann's paper "on the relationship between second fundamental theorem of the mechanical theory of heat and probability calculations regarding the conditions for thermal equilibrium" *Sitzungsberichte der Kaiserlichen Akademie der Wissenschaften. Mathematisch-Naturwissen Classe. Abt II, LXXVI 1877*, pp 373–435 *Entropy* 17:1971–2009.
27. Xu X, Ge R, Li L, Wang J, Lu X, Xue S, Chen X, Li Z and Bian J (2018) Exploring the tetrahydroisoquinoline thiohydantoin scaffold blockade of the androgen receptor as potent anti-prostate cancer agents. *Eur. J. Med. Chem* 143:1325–1344. [PubMed: 29117897]
28. Harrison JR, O'Brien P, Porter DW and Smith NM (1999) Studies towards the preparation of spartine-like diamines for asymmetric synthesis. *J. Chem. Soc* 24:3623–3631.
29. Marenich AV and Truhlar DG (2009) Universal solvation model based on solute electron density and on a continuum model of solvent defined by the bulk dielectric constant and atomic surface tensions. *J. Phys. Chem. B* 113:6378–6396. [PubMed: 19366259]
30. Grimblat N and Sarotti AM (2016) Computational chemistry to the rescue: modern toolboxes for the assignment of complex molecules by GIAO NMR calculations. *Chem. Eur. J* 22:12246–12261. [PubMed: 27405775]
31. Adamo C and Barone V (1998) Exchange functionals with improved long-range behavior and adiabatic connection methods without adjustable parameters: The mPW and mPW1PW models. *J. Chem. Phys* 108:664–675.
32. Lodewyk MW, Siebert MR and Tantillo DJ (2012) Computational prediction of <sup>1</sup>H and <sup>13</sup>C chemical shifts: a useful tool for natural products, mechanistic, and synthetic organic chemistry. *Chem. Rev* 112:1839–1862. [PubMed: 22091891]
33. Willoughby PH, Jansma MJ and Hoye TR (2014) A guide to small-molecule structure assignment through computation of (<sup>1</sup>H and <sup>13</sup>C) NMR chemical shifts. *Nat. Protoc* 9:643–660. [PubMed: 24556787]
34. Van der Plas SE, Kelgtermans H, De Munck T, Martina SLX, Dropsit S, Quinton E, De Blicke A, Joannesse C, Tomaskovic L, Jans M, Christophe T, Van der Aar E, Borgonovi M, Nelles L, Gees M, Stouten PFW, Van Der Schueren J, Mammoliti O, Conrath K and Andres MJ (2018) Discovery of N-(3-carbamoyl-5,5,7,7-tetramethyl-5,7-dihydro-4H-thieno[2,3-c]pyran-2-yl)-1H-pyrazole-5-carboxamide (GLPG1837), a novel potentiator which can open class III mutant cystic fibrosis transmembrane conductance regulator (CFTR) channels to a high extent. *J. Med. Chem* 61:1425–1435. [PubMed: 29148763]
35. Yeh HI, Qui L, Sohma Y, Conrath K, Zou X and Hwang TC (2019) Identifying the molecular target sites for CFTR potentiators GLPG1837 and VX-770. *J. Gen. Physiol* 151:912–928. [PubMed: 31164398]
36. Liu F, Zhang Z, Levit A, Levring J, Touhara KK, Shoichet BK and Chen J (2019) Structural identification of a hotspot on CFTR for potentiation. *Science* 364:1184–1188. [PubMed: 31221859]
37. Molinski SV, Gonska T, Huan LJ, Baskin B, Janahi IA, Ray PN and Bear CE (2014) Genetic, cell biological, and clinical interrogation of the CFTR mutation c.3700 A>G (p.Ile1234V) informs of strategies for future medical intervention. *Genetics Med.* 16:625–632. [PubMed: 24556927]
38. Molinski SV, Ahmadi S, Ip W, Ouyang H, Vilella A, Miller JP, Lee P-S, Kulleperuma K, Du K, Di Paola M, Eckford PDW, Laselva O, Huan LJ, Wellhauser L, Li E, Ray PN, Pomes R, Moraes T, Gonska T, Ratjen F and Bear CE (2017) Orkambi and amplifier co-therapy improves function from a rare CFTR mutation in gene-edited cells and patient tissue. *EMBO Mol. Med* 9:1224–1243. [PubMed: 28667089]

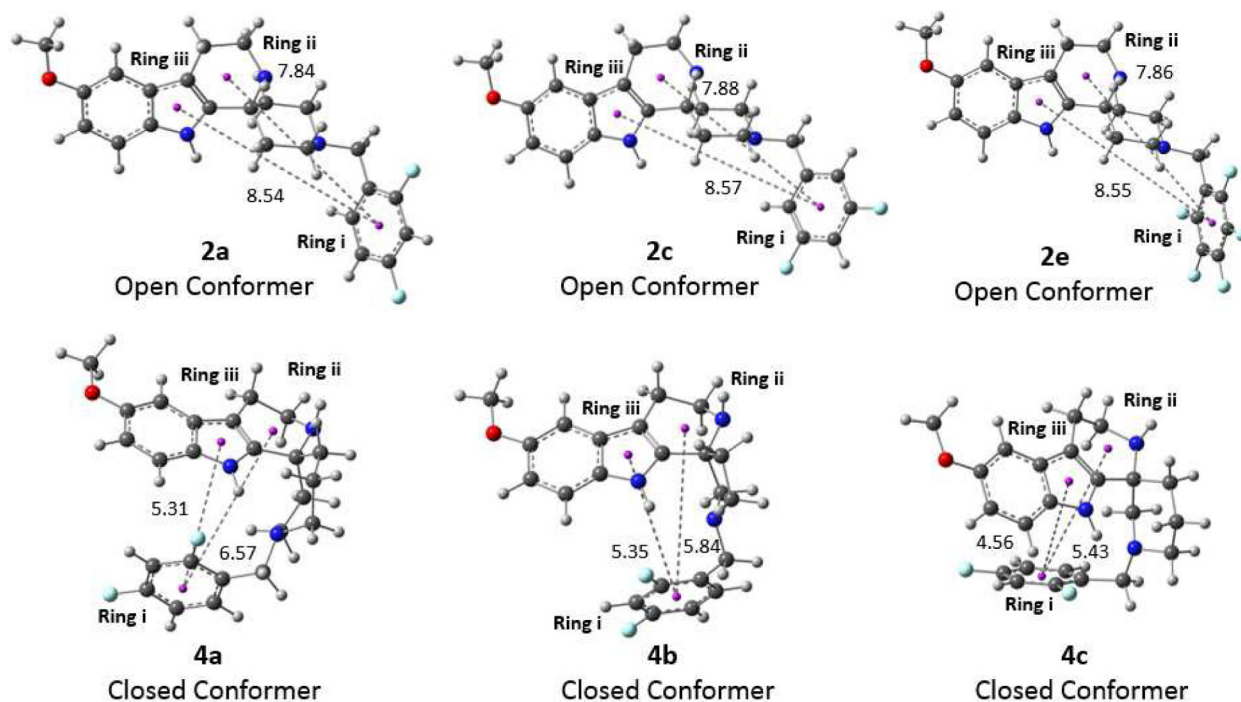
39. Valley HC, Bukis KM, Bell A, Cheng Y, Wong E, Jordan NJ, Allaire NE, Sivachenko A, Liang F, Bihler H, Thomas PJ, Mahlou J and Mense M (2018) Isogenic cell models of cystic-fibrosis-causing variants in natively expressing pulmonary epithelial cells. *J. Cyst. Fibros* 18:476–483. [PubMed: 30563749]
40. Sharma J, Keeling KM and Rowe SM (2020) Pharmacological approaches for targeting cystic fibrosis nonsense mutations. *Eur. J. Med. Chem* 299:epub.

**HIGHLIGHTS:**

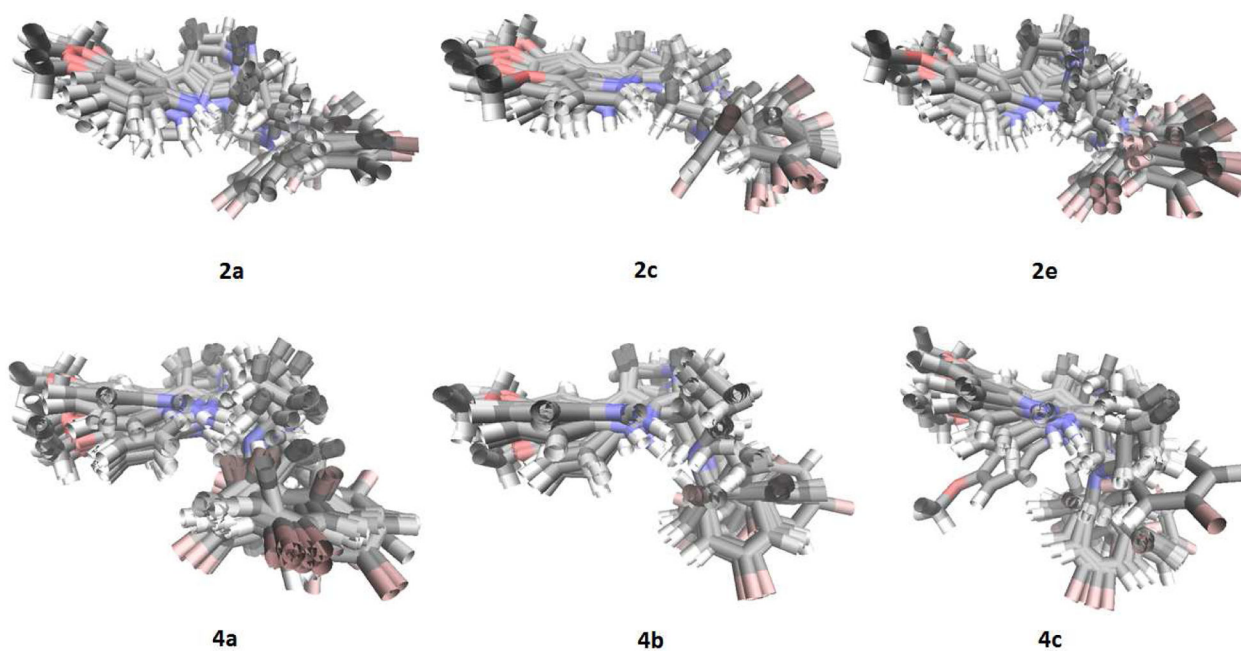
- Approximately 10% of cystic fibrosis subject remain without CFTR modulator therapy
- Co-potentiators represent a novel class of CFTR modulators
- Co-potentiators act in synergy with potentiators to activate rare CFTR mutants
- Spiro[piperidine-4,1-pyrido[3,4-b]indole] co-potentiators were optimized by structure-activity studies
- Spiro[piperidine-4,1-pyrido[3,4-b]indoles] with EC<sub>50</sub> down to 600 nM, an approximately 17-fold improvement, were identified



**Figure 1.**  
Structural variants 1–6 of the spiro[piperidine-4,1'-pyrido[3,4-*b*]indole] scaffold.

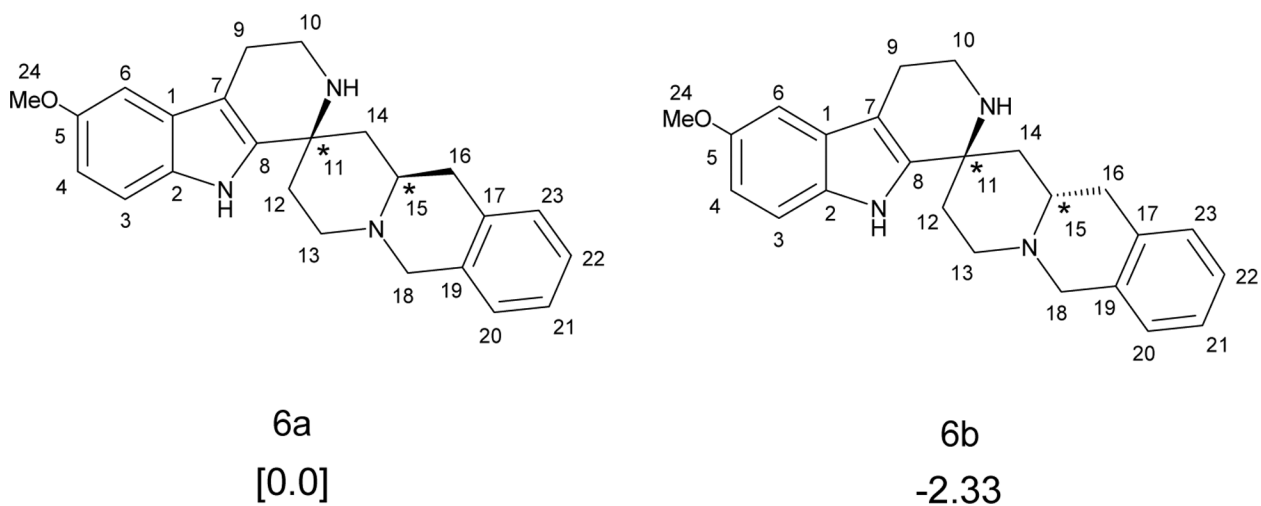


**Figure 2.** Optimized geometries of the lowest energy conformers of **2a**, **2c**, **2e** and **4a–4c**. Distances (Å) are measured from the centroid of *Ring i*, to those of *Ring ii* and *Ring iii*. The lowest energy conformers for **4a–c** preferred a close form conformation, where one face of *Ring i* is blocked from potential interactions with the protein interior.

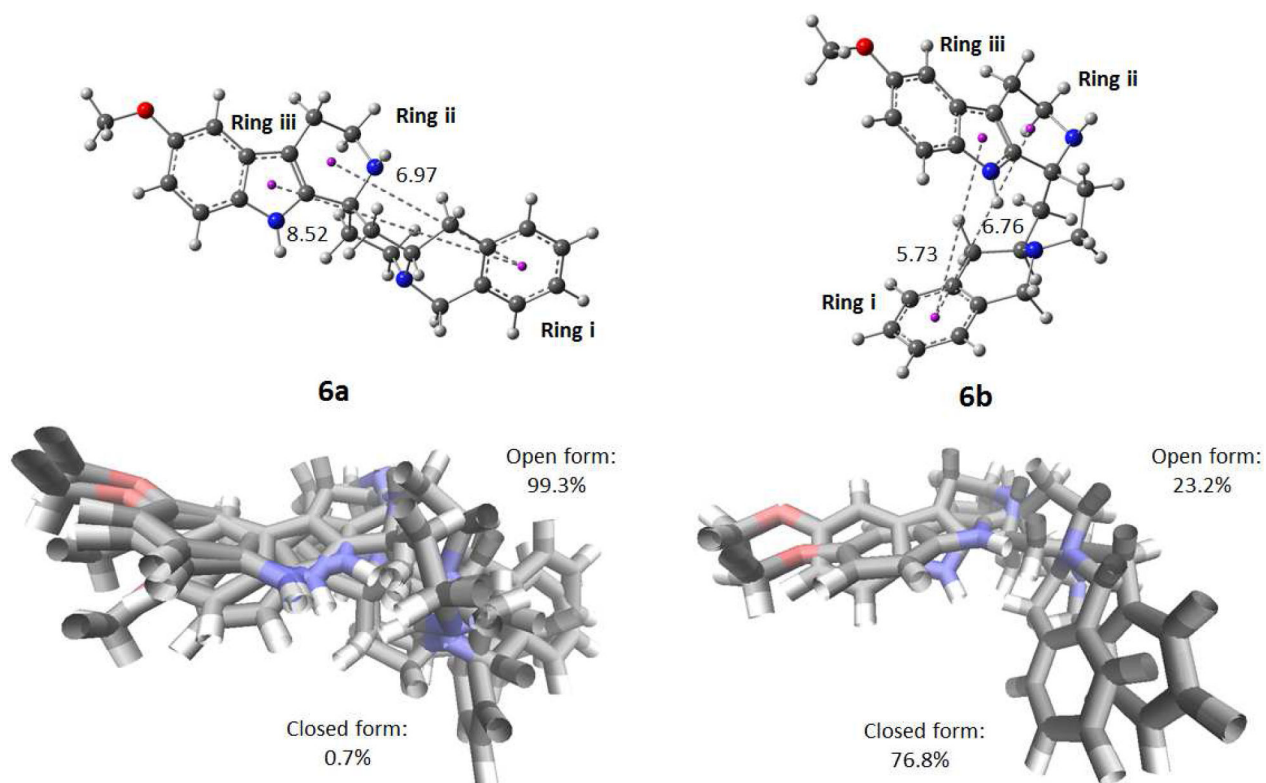


**Figure 3.**  
Superposition of optimized energetically relevant conformers for **2a**, **2c**, **2e**, **4a-4c**.

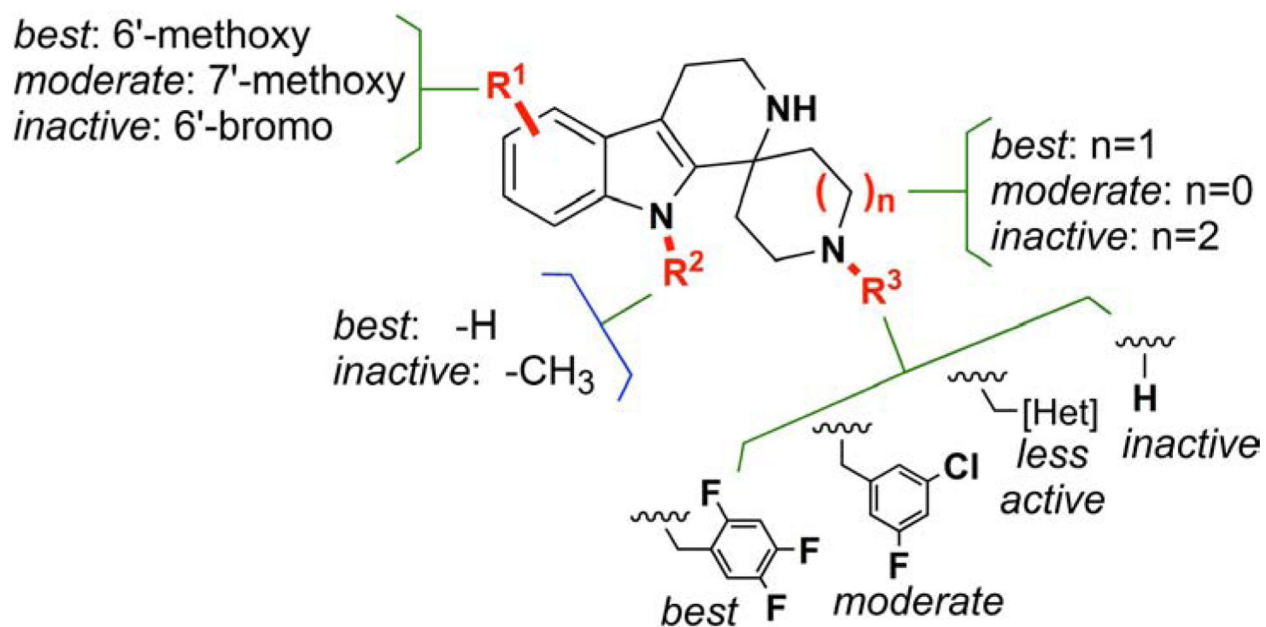




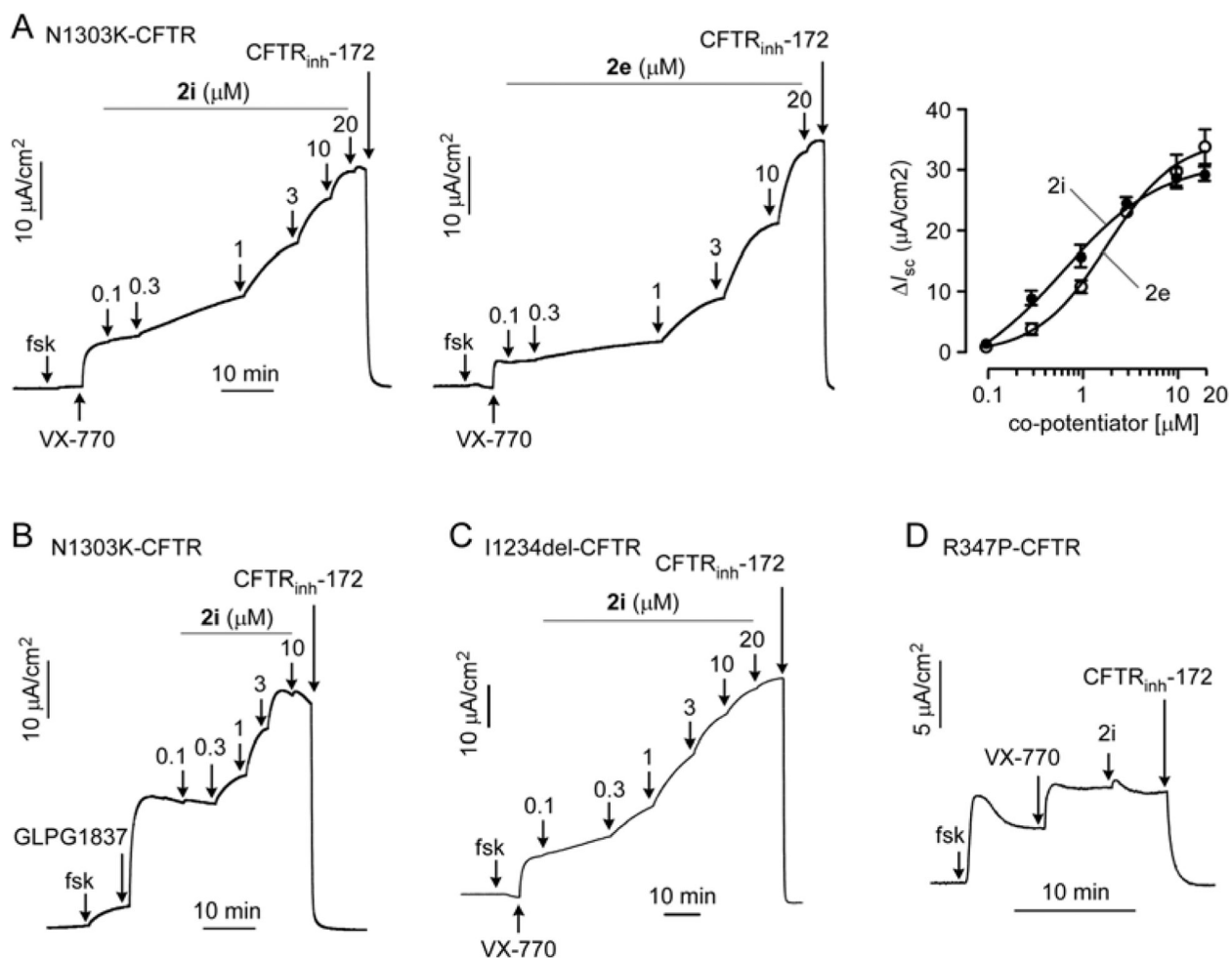
**Figure 4.** Structures of **6a** and **6b**. Based on quantum calculations at SMD(chloroform)-B3LYP-D3(BJ)/6-31+G(d,p). **6b** is 2.33 kcal/mol more thermodynamically favorable than **6a**.



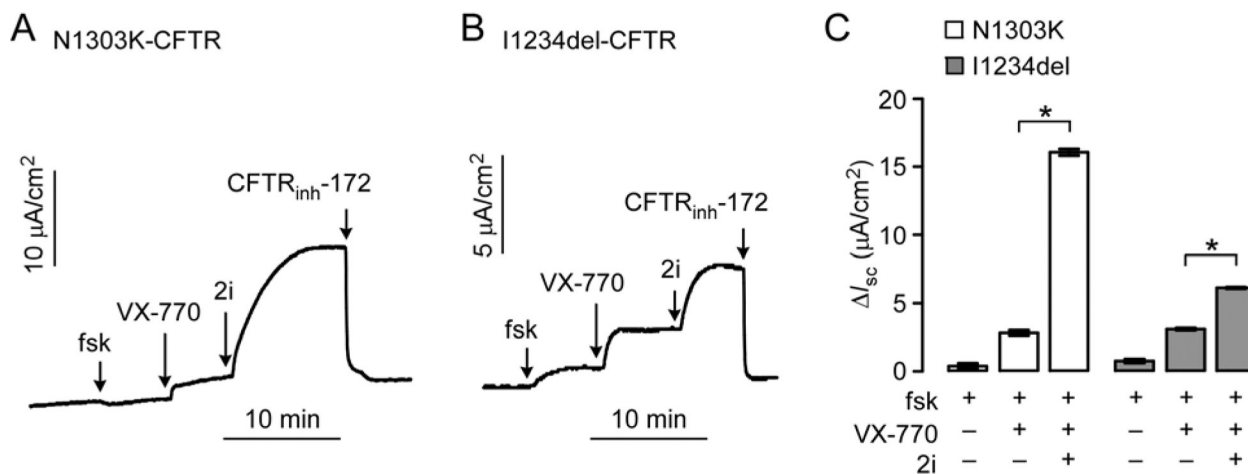
**Figure 5.** Lowest energy conformers optimized at SMD(chloroform)6-31+G(d,p) with D3(BJ) for **6a** and **6b** respectively (top); the distance between centroids of *Rings i* and *ii* and *Rings i* and *iii* were measured. Superimposed images of energetically relevant conformers for **6a** and **6b** (bottom); **6a** has more open form conformers in equilibrium.



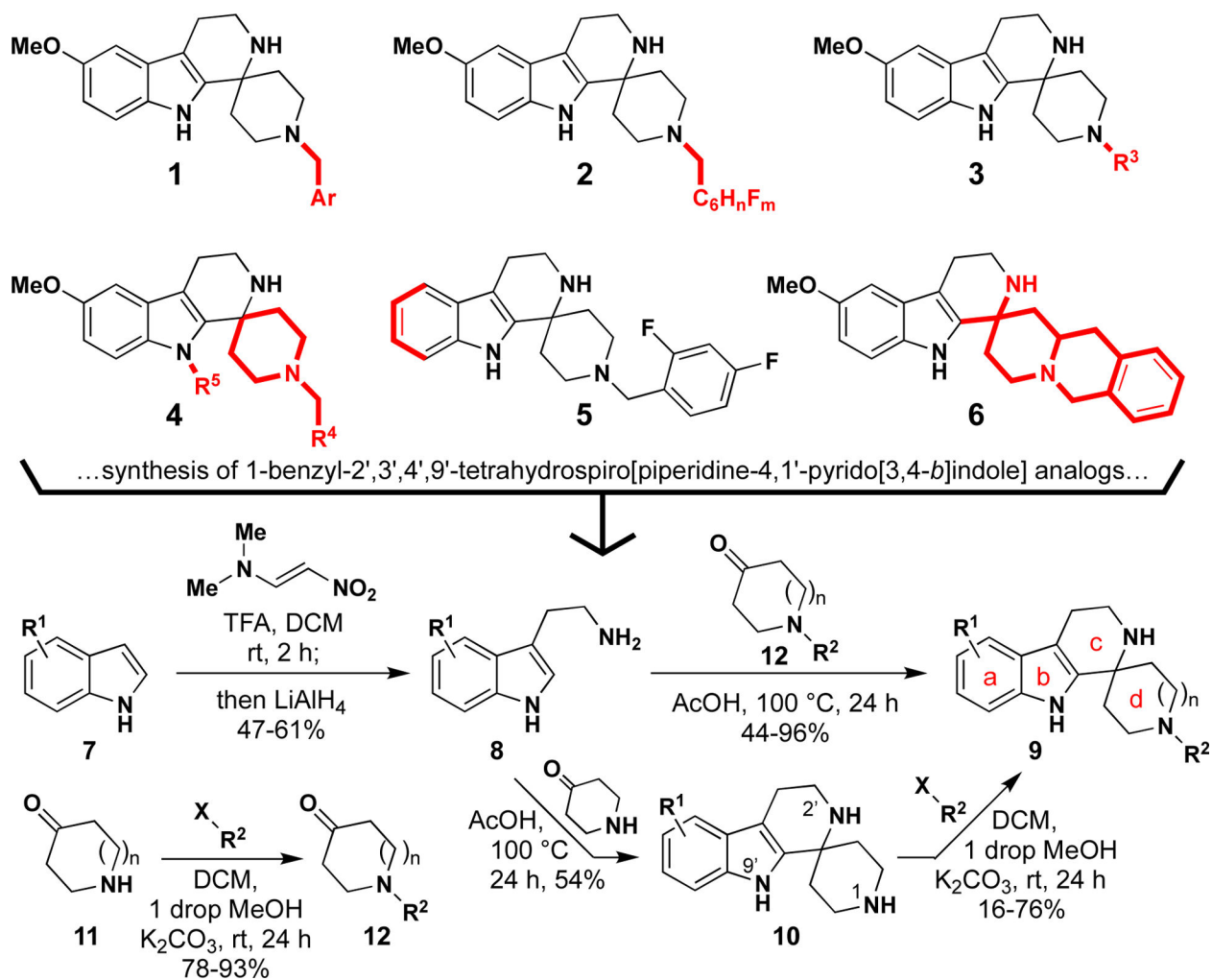
**Figure 6.** Structural determinants of spiro[piperidine-4,1'-pyrido[3,4-*b*]indole] scaffold. See text for explanation.



**Figure 7.** Short-circuit current measurement of mutant CFTR activation by spiro[piperidine-4,1-pyrido[3,4-b]indoles]. *A. (left)* Short-circuit current data in FRT cells expressing N1303K-CFTR in response to 20 μM forskolin (fsk), 5 μM VX-770, indicated concentration of **2i** and **2e**, and 10 μM CFTR<sub>inh</sub>-172. *(right)* Summary of concentration-dependence data (n=3, mean ± S.E.M.). *B.* Measurements done as in A, but with 20 μM GLPG1837 instead of VX-770. *C.* Short-circuit current in FRT cells expressing I1234del-CFTR in response to 20 μM forskolin, 5 μM VX-770, indicated concentration of **2i**, and 10 μM CFTR<sub>inh</sub>-172. *D.* Short-circuit current in FRT cells expressing R347P-CFTR in response to 20 μM forskolin, 5 μM VX-770, 20 μM **2i** and 10 μM CFTR<sub>inh</sub>-172. In all studies, cells were corrected with 3 μM VX-661 for 18–24 hours prior to measurement. All traces are representative of three replicates.

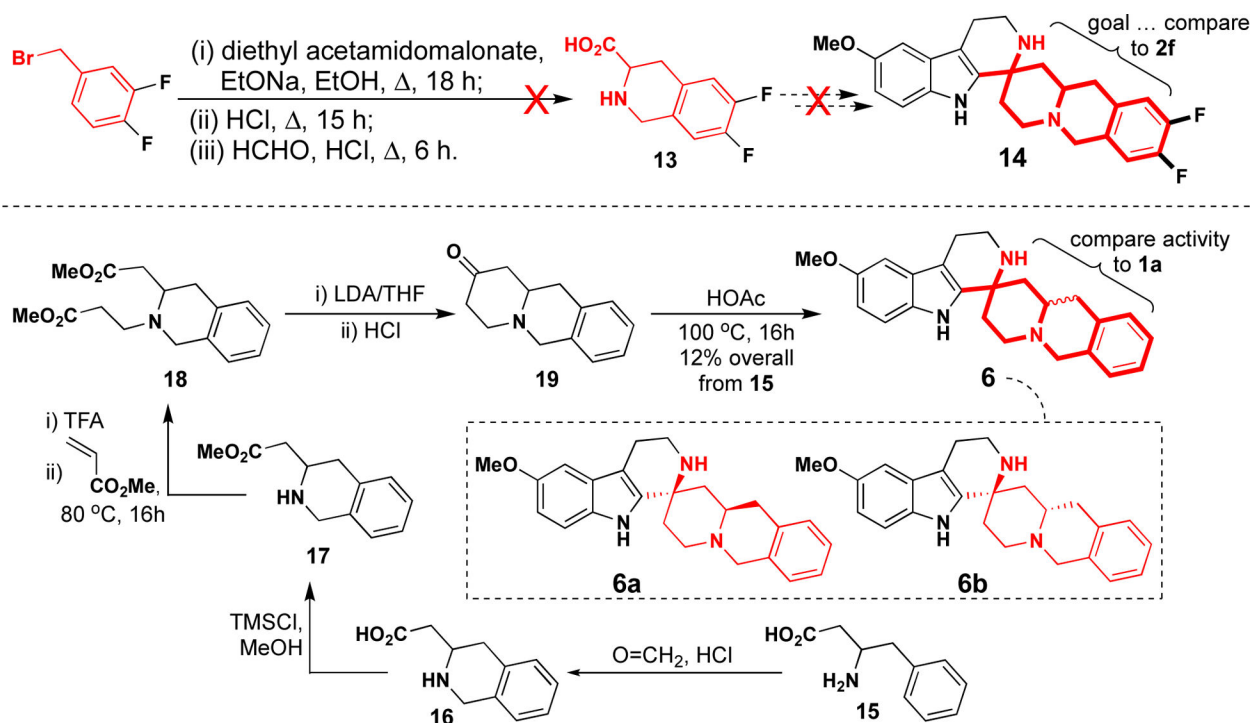


**Figure 8.** Activity of **2i** in human airway epithelial cell cultures. *A.* Short-circuit current in gene-edited 16HBE14o- cells expressing N1303K-CFTR. *B.* Short-circuit current data in gene-edited 16HBE14o- cells expressing I1234del-CFTR. *C.* Summary of changes in short-circuit current ( $\Delta I_{sc}$ ; mean  $\pm$  S.E.M.,  $n = 3$ ,  $*P < 0.05$ ). Concentrations: 20  $\mu M$  forskolin, 5  $\mu M$  VX-770, 10  $\mu M$  **2i**, and 10  $\mu M$  CFTR<sub>inh</sub>-172. 16HBE14o- cell models expressing I1234del-CFTR were corrected with 18  $\mu M$  VX-661 and 3  $\mu M$  VX-445 for 18–24 hours prior to measurement.



Scheme #1.

Synthetic route to spiro[piperidine-4,1'-pyrido[3,4-*b*]indole] analogs 1–6.



**Scheme #2.**  
 Synthesis of constrained analog **6**.



**Table 1.**

Predicted Boltzmann distributions for Open vs. Closed forms for 2a, 2c, 2e, and 4a–4c at (PCM)chloroform-B3LYP-D3(BJ)//6-31+G(d,p) (left) and (PCM)chloroform-B3LYP-D3(BJ)//6-311+G(2d,2p) (right).

Structures	Free Energy at PCM-(chloroform)-B3LYP-D3(BJ)//6-31+G(d,p)		Electronic Energy at PCM-(chloroform)-B3LYP-D3(BJ)//6-311+G(2d,2p)	
	Boltzmann Weight for Open form	Boltzmann Weight for Closed Form	Boltzmann Weight for Open form	Boltzmann Weight for Closed Form
2a	99.5%	0.5%	89.6%	10.4%
2c	98.7%	1.3%	96.7%	3.3%
2e	98.9%	1.1%	94.5%	5.5%
4a	3.7%	96.3%	1.7%	98.3%
4b	6.1%	93.9%	7.7%	92.3%
4c	2.9%	97.1%	1.7%	98.3%

Author Manuscript

Author Manuscript

Author Manuscript

Author Manuscript

Table 2.

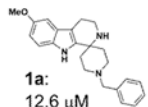
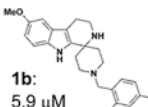
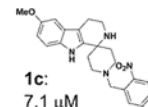
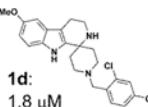
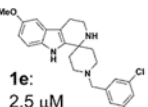
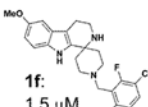
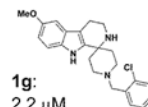
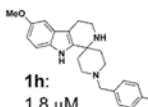
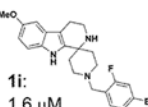
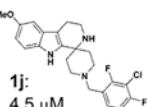
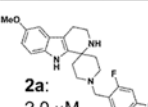
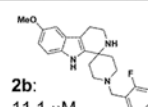
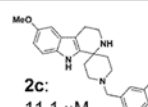
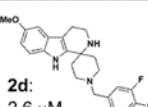
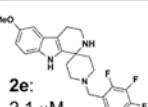
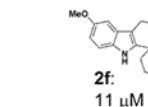
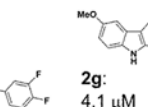
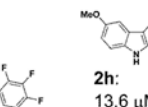
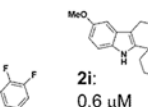

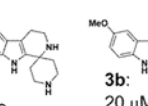
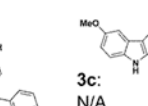
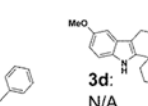

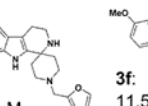
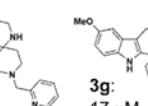
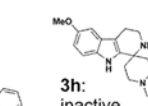
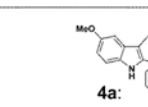
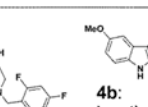
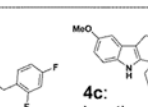
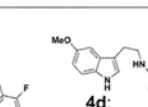
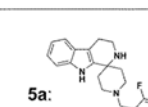
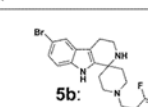
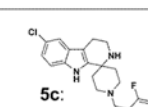
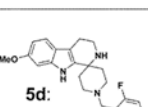
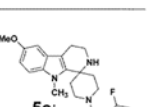
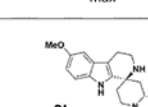
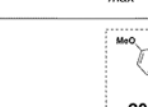
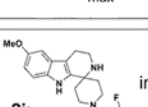
Calculated  $^{13}\text{C}$  and  $^1\text{H}$  chemical shifts for **6a** and **6b**, and their deviation from experiments.

Atom Label	Exp. $^{13}\text{C}$ <b>6</b> (p.p.m)	Calculated <b>6a</b> shift	Dev.	Calculate d <b>6b</b> shift	Dev.	Exp. $^1\text{H}$ <b>6</b> (p.p.m)	Calculated <b>6a</b> shift	Dev.	Calculated <b>6b</b> shift	Dev.
1	128.10	129.08	0.98	130.04	1.94	---	---	---	---	---
2	130.74	130.14	0.60	129.69	1.05	---	---	---	---	---
3	111.62	109.53	2.09	109.80	1.82	7.06	7.19	0.14	6.79	0.26
4	100.46	103.28	2.82	102.43	1.97	6.78	6.72	0.06	6.60	0.18
5	153.98	153.72	0.26	153.66	0.32	---	---	---	---	---
6	108.47	103.35	5.12	103.45	5.02	6.94	6.92	0.02	6.92	0.02
7	111.46	109.05	2.41	105.97	5.49	---	---	---	---	---
8	140.49	142.89	2.40	143.23	2.74	---	---	---	---	---
9	23.26	24.11	0.85	24.08	0.82	2.71	2.52	0.19	2.55	0.16
						2.71	2.59	0.12	2.62	0.09
10	43.76	39.56	4.21	40.94	2.82	3.08	2.94	0.14	3.07	0.01
						3.08	2.98	0.10	3.21	0.13
11	52.91	53.93	1.02	53.82	0.91	---	---	---	---	---
12	26.37	34.96	1.41	37.20	0.83	2.00	2.02	0.02	2.25	0.25
						1.88	1.79	0.08	1.72	0.15
13	50.40	43.27	<b>7.13</b>	48.26	2.13	2.94	3.06	0.12	2.90	0.04
						2.62	2.38	0.24	2.66	0.04
14	39.28	40.98	1.70	38.35	0.93	2.25	2.29	0.04	2.04	0.21
						1.88	1.53	0.34	1.88	0.15
15	56.05	52.83	3.22	56.32	0.27	2.88	3.26	<b>0.38</b>	2.76	0.12
16	36.64	29.75	5.89	35.51	0.13	2.62	2.41	0.21	2.38	0.24
						2.71	4.02	<b>1.31</b>	2.46	0.25
17	133.42	135.31	1.89	136.74	3.31	---	---	---	---	---
18	57.58	56.39	1.19	56.81	0.77	3.52	3.69	0.17	3.50	0.00
						3.86	4.22	<b>0.36</b>	3.86	0.02
19	133.80	135.63	1.83	136.99	3.19	---	---	---	---	---
20	126.02	126.24	0.22	126.36	0.34	7.06	7.15	0.09	7.24	0.18
21	125.81	125.98	0.17	125.82	0.01	7.11	7.10	0.01	7.14	0.03
22	126.40	126.37	0.02	126.86	0.46	7.14	7.12	0.02	7.18	0.04
23	127.67	128.94	1.27	129.60	1.93	7.06	7.16	0.10	6.99	0.06
24	51.35	53.17	1.82	53.14	1.79	3.86	3.67	0.19	3.56	0.30
<b>MAD</b>			2.11		1.71			0.19		0.12

\* Abbreviation: MAD, mean absolute deviation; and Dev., deviation. Deviations of less than 6 ppm for  $^{13}\text{C}$  and less than 0.3 ppm for  $^1\text{H}$  shifts are considered acceptable [30, 32, 33]. Chemical shifts exceeding the accepted deviations are bolded above. Coupling constants (J) were also calculated to confirm the identity of complex proton peaks (see SI for details).

Table 3.

## Bioassay results.

 <b>1a:</b> 12.6 $\mu\text{M}$ 54% $V_{\text{max}}$	 <b>1b:</b> 5.9 $\mu\text{M}$ 101% $V_{\text{max}}$	 <b>1c:</b> 7.1 $\mu\text{M}$ 111% $V_{\text{max}}$	 <b>1d:</b> 1.8 $\mu\text{M}$ 79% $V_{\text{max}}$	 <b>1e:</b> 2.5 $\mu\text{M}$ 97% $V_{\text{max}}$
 <b>1f:</b> 1.5 $\mu\text{M}$ 61% $V_{\text{max}}$	 <b>1g:</b> 2.2 $\mu\text{M}$ 63% $V_{\text{max}}$	 <b>1h:</b> 1.8 $\mu\text{M}$ 80% $V_{\text{max}}$	 <b>1i:</b> 1.6 $\mu\text{M}$ 58% $V_{\text{max}}$	 <b>1j:</b> 4.5 $\mu\text{M}$ 120% $V_{\text{max}}$
 <b>2a:</b> 2.0 $\mu\text{M}$ 100% $V_{\text{max}}$	 <b>2b:</b> 11.1 $\mu\text{M}$ 63% $V_{\text{max}}$	 <b>2c:</b> 11.1 $\mu\text{M}$ 63% $V_{\text{max}}$	 <b>2d:</b> 2.6 $\mu\text{M}$ 121% $V_{\text{max}}$	 <b>2e:</b> 2.1 $\mu\text{M}$ 134% $V_{\text{max}}$
 <b>2f:</b> 11 $\mu\text{M}$ 7% $V_{\text{max}}$	 <b>2g:</b> 4.1 $\mu\text{M}$ 100% $V_{\text{max}}$	 <b>2h:</b> 13.6 $\mu\text{M}$ 94% $V_{\text{max}}$	 <b>2i:</b> 0.6 $\mu\text{M}$ 97% $V_{\text{max}}$	
 <b>3a:</b> inactive	 <b>3b:</b> 20 $\mu\text{M}$ 100% $V_{\text{max}}$	 <b>3c:</b> N/A 4% $V_{\text{max}}$	 <b>3d:</b> N/A 17% $V_{\text{max}}$	
 <b>3e:</b> 16.4 $\mu\text{M}$ 67% $V_{\text{max}}$	 <b>3f:</b> 11.5 $\mu\text{M}$ 107% $V_{\text{max}}$	 <b>3g:</b> 17 $\mu\text{M}$ 56% $V_{\text{max}}$	 <b>3h:</b> inactive	
 <b>4a:</b> 20 $\mu\text{M}$ 12% $V_{\text{max}}$	 <b>4b:</b> inactive	 <b>4c:</b> inactive	 <b>4d:</b> inactive	
 <b>5a:</b> 8.2 $\mu\text{M}$ 100% $V_{\text{max}}$	 <b>5b:</b> 21 $\mu\text{M}$ 92% $V_{\text{max}}$	 <b>5c:</b> 2.5 $\mu\text{M}$ 89% $V_{\text{max}}$	 <b>5d:</b> 2.4 $\mu\text{M}$ 100% $V_{\text{max}}$	 <b>5e:</b> inactive
 <b>6b:</b> inactive	 <b>20:</b> 10 $\mu\text{M}$ original high through-put lead		 <b>2i:</b> 0.6 $\mu\text{M}$ new lead: ~17 fold improvement	

Biology: Characterization of spiro[piperidine-4,1-pyrido[3,4-b]indoles] co-potentiators